Phosphoglycolate has profound metabolic effects but most likely no role in a metabolic DNA response in cancer cell lines.

Isabelle Gerin*, Marina Bury*, Francesca Baldin, Julie Graff, Emile Van Schaftingen, Guido T. Bommer.

de Duve Institute and WELBIO, UCLouvain, Avenue Hippocrate 75, 1200 Bruxelles, Belgium

Correspondence should be addressed to: guido.bommer@uclouvain.be

* These authors contributed equally to this work.

ABSTRACT

Repair of a certain type of oxidative DNA damage leads to the release of phosphoglycolate, which is an inhibitor of triose phosphate isomerase and is predicted to indirectly inhibit phosphoglycerate mutase activity. Thus, we hypothesized that phosphoglycolate might play a role in a metabolic DNA damage response. Here, we determined how phosphoglycolate is formed in cells, elucidated its effects on cellular metabolism and tested whether DNA damage repair might release sufficient phosphoglycolate to provoke metabolic effects.

Phosphoglycolate concentrations were below 5 μM in wild type U2OS and HCT116 cells, and remained unchanged when we inactivated phosphoglycolate phosphatase (PGP), the enzyme that is believed to dephosphorylate phosphoglycolate. Treatment of PGP knockout cell lines with glycolate caused an up to 500-fold increase in phosphoglycolate concentrations, which resulted largely from a side-activity of pyruvate kinase. This increase was much higher than in glycolate-treated wild type cells and was accompanied by metabolite changes consistent with an inhibition of phosphoglycerate mutase, most likely due to the removal of the priming phosphorylation of this enzyme. Surprisingly, we found that phosphoglycolate also inhibits succinate dehydrogenase with a Ki of < 10 μM. Thus, phosphoglycolate can lead to profound metabolic disturbances.

In contrast, phosphoglycolate concentrations were not significantly changed when we treated PGP knockout cells with Bleomycin or ionizing radiation, which are known to lead to the release of phosphoglycolate by causing DNA damage. Thus, phosphoglycolate concentrations due to DNA damage are too low to cause major metabolic changes in HCT116 and U2OS cells.

INTRODUCTION

Phosphoglycolate can be formed in all organisms during the repair of DNA damage. Oxidative stress or treatment with certain chemotherapeutic drugs (e.g. Bleomycin) and ionizing radiation leads to the oxidative cleavage of deoxyribose moieties, resulting in DNA 3' ends that carry a phosphoglycolate group [1]. These 3'-phosphoglycolate groups can be removed either by releasing phosphoglycolate (via the enzyme APE1, [2-4]) or by releasing glycolate (via the enzyme TDP1, [5-7]) (see **Suppl. Fig. 1A**). Phosphoglycolate is known to have an effect on two steps in glycolysis. On the one hand, it is an inhibitor of triose phosphate isomerase with a Ki of approximately 20 μM [8-10]. On the other hand, phosphoglycolate is expected to indirectly inhibit the activity of phosphoglycerate mutases, by stimulating the hydrolysis of the "priming phosphorylation" of the enzyme [11, 12]. This indicates that the link between phosphoglycolate release and metabolic changes could represent an ancient direct metabolic stress response, which might collaborate with more indirect effects of DNA damage on cellular metabolism [13, 14] (**Suppl. Fig. 1A**).

Two lines of evidence in the literature suggest a role of phosphoglycolate in the cellular response to oxidative stress. The first one is the observation that murine embryonic fibroblasts proliferate significantly slower upon inactivation of the enzyme phosphoglycolate phosphatase (PGP)[15], which is the enzyme that is believed to eliminate phosphoglycolate in cells. This difference was abolished under hypoxic conditions. Phosphoglycolate is expected to be formed by oxidative DNA damage and should accumulate to higher levels in PGP knockout cells than in wild type cells. It was therefore tempting to speculate that increased concentrations of phosphoglycolate might play a role in the growth inhibition and some data was presented in support of this hypothesis [15] (see below).

The second line of evidence is the observation that reversible oxidation of PGP (also called AUM) can inhibit its activity and change its oligomerization state [16]. This suggests that under some conditions of oxidative stress, the elimination of phosphoglycolate by PGP might be compromised.

Taken together, oxidative stress might increase phosphoglycolate both at the level of its production (i.e. by promoting DNA damage) and at the level of its elimination (i.e. by inhibiting the enzyme PGP).

Unfortunately, the link between phosphoglycolate accumulation and the inhibition of cellular proliferation might not be quite as direct. When investigating the role of phosphoglycolate in the growth defect of PGP mutant MEFs, researchers used an inhibitor of the enzyme TDP1 to reduce phosphoglycolate levels. TDP1 is indeed one of the enzymes that

cleans up 3'-phosphoglycolate-DNA ends. Yet, this enzyme removes glycolate and not phosphoglycolate from DNA ends [5-7]. Therefore, inhibition of TDP1 is not expected to decrease phosphoglycolate concentrations, but might rather increase phosphoglycolate concentrations since remaining 3'-phosphoglycolate-DNA ends could be processed by the enzyme APE1 (which actually leads to a release of phosphoglycolate)[3]. Thus, the observation that treatment with a TDP1 inhibitor rescues growth of PGP mutant MEFs, does not support the notion that the growth inhibition is caused by phosphoglycolate but rather indicates that the cause for the growth inhibition in PGP mutant MEFs is likely more complex than previously assumed.

To make things even more complicated, the link between PGP and phosphoglycolate metabolism is less obvious than the name of this enzyme might suggest. Since its first description in 1977 [17], PGP has been described as a phosphatase that is most active on phosphoglycolate. While phosphoglycolate is abundant in plants, where it is formed as a side-product of the enzyme Rubisco, in mammals phosphoglycolate is not part of any known metabolic pathway, but is primarily thought to be released during the repair of DNA damage.

Three lines of evidence suggest that the activity on phosphoglycolate might not be the most important function of PGP: First, we have recently shown that PGP plays a key role in cellular metabolism by eliminating two glycolytic side products, that otherwise interfere with glycolysis and the pentose phosphate pathway [18] (**Suppl. Fig. 1B**). On the one hand, PGP eliminates 4-P-erythronate, which can be formed when the glycolytic enzyme glyceraldehyde-3-phosphate-dehydrogenase (GAPDH) erroneously acts on erythrose 4-phosphate. On the other hand, PGP destroys also L-2-P-lactate, which can be formed when pyruvate kinase erroneously acts on L-lactate. Elimination of both metabolites is important, since 4-P-erythronate is a potent inhibitor (Ki < 1 μM) of the pentose phosphate pathway enzyme 6-P-gluconate dehydrogenase, and 2-P-lactate is a strong inhibitor of enzymes that synthesize the glycolytic activator fructose 2,6-bisphosphate. As expected, inactivation of PGP in cancer cells caused 10 to 50-fold increases in 4-P-erythronate and 2-P-lactate, as well as profound secondary disturbances including an inhibition of the glycolytic flux, a more than 100-fold increase in 6-P-gluconate concentration and reduced cell proliferation [18].

Second, it has been reported that a low activity of PGP on 3-P-glycerol is sufficient to modulate concentrations of this metabolite and might play a role in regulating cellular lipid metabolism [19, 20].

Last but not least, while knockout out or knock-down of PGP in mammalian cells has dramatic effects on 4-P-erythronate, 2-P-lactate and in some studies moderate effects on

glycerol-3-phosphate [15, 18-20], we were surprised not to detect any increase in phosphoglycolate beyond background levels in our previous study [18].

Here, we wanted to investigate how phosphoglycolate is formed in cells, what metabolic changes its accumulation can provoke and whether phosphoglycolate released during DNA repair might lead to noticeable metabolic changes.

EXPERIMENTAL

Lentiviral constructs

Lentiviral constructs driving expression of *E. coli* gpmI were generated by inserting a PCR fragment (forward: ATA CAT AGC TAG CCA CCA TGT TGG TTT CTA AAA AAC CTA TG, reverse: TATAATGTACATTATTCCACGATGAACAGC) between the restriction sites NheI and BsrGI in the plasmid pOH425 [21]. The mouse Glyctk open reading frame was originally amplified from mouse liver cDNA and inserted into a prokaryotic expression vector. The open reading frame was then amplified by PCR and inserted into the plasmid pOH425 (details are available upon request). Inserts for the generation of lentiviral shRNA constructs were produced by amplifying synthetic oligonucleotides (IDT) (supplementary table 1) in a PCR reaction with Phusion high fidelity polymerase as described using primers TGA ACT CGA GAA GGT ATA TTG CTG TTG ACA GTG AGC G and TCT CGA ATT CTA GCC CCT TGA AGT CCG AGG CAG TAG GC [22]. Resulting PCR products were inserted via the restriction sites XhoI and EcoRI into an optimized miR-30 scaffold behind a turbo GFP expression cassette. This vector is similar to the constructs described by Fellmann and colleagues [22], but based on the vector pLVX-PURO (Clontech). Details about the construction of this vector are available upon request.

Cell culture and lentiviral transduction

Cell lines were cultured in DMEM medium containing 4.5 $g.l^{-1}$ D-glucose, 10 % foetal calf serum, 2 mM Ultraglutamine I (Lonza), and 100 $U.ml^{-1}$ Penicillin/Streptomycin (Lonza). PGP knockout cell lines were described before [23]. Knockout cell lines in HCT116 cells (rescued or not with mouse PGP) were described before [18]. The U2OS PGP knockout cell line was generated using the same approach as before [18]. To inactivate the PGP gene in polyclonal populations of the immortalized human fibroblast cell line HFF2-tert [24] (a generous gift of Anabelle Decottignies, UCLouvain, Belgium) we used the plasmid lentiCRISPR V2. Sequences of guide RNAs targeting human PGP or lacZ were inserted by ligating annealed

oligonucleotides (see **Suppl. table 1**) into the BsmBI site of this vector [25]. To generate recombinant lentiviruses (for overexpression of gpmI, knockdown of PKM/GLYCTK or lentiviral knockout of PGP), HEK293 T cells were transiently transfected with lentiviral vectors and second generation packaging plasmids psPAX2 and pMD2.G (kind gifts of Didier Trono, Addgene #12260 and #12259) using the calcium phosphate coprecipitation method as described before [26, 27]. 24 h after transfection, target cells were infected in the presence of 8 μ g.ml^{-1} polybrene (Sigma). Infected cells were selected for 4 days with 1.5 μ g.ml^{-1} of puromycin (Thermofisher), 300 μ g.ml^{-1} of hygromycin (Invivogen).

For the treatment with glycolate, glycolic acid (Sigma) was neutralized with sodium hydroxide and subsequently added to the medium at the indicated concentrations. Deuterated glycolate was synthesised by reduction of glyoxylic acid with sodium borodeuteride. To this end, the two compounds were mixed at equimolar concentration and kept overnight at room temperature under basic pH. The mixture was neutralized with hydrochloric acid and stored at -20 °C. A control solution was made by mixing glyoxylic acid and sodium borohydride to form non-labelled glycolate.

Before the induction of DNA damage, cells were plated at 400,000 and 300,000 cells per well of a six-well plate for HCT116 and U2OS cells, respectively, and let grow overnight. The following day, medium was replaced by medium containing 10 % v/v foetal bovine serum, 2 mM L-glutamine and 20 mM D-glucose. Cells were treated with 0, 5, 20 or 50 µM Bleomycin (Santa Cruz, Heidelberg, Germany) or 5 Gray from a ^{137}Cs source 24 h, 8 h, 4 h and 0.5 h before harvesting the cells on the next day. As a positive control, where indicated, we added 5 mM glycolate 6 h before harvesting.

Determination of the Ki for succinate dehydrogenase and enolase

Succinate dehydrogenase activity was assessed on rat liver mitochondria and on mitochondria obtained from PGP wild type and knockout HCT116 cell lines. To this end, we isolated mitochondria as described before [28] (after approval by the animal ethics commitee of the medical faculty of the UCLouvain). Briefly, the liver from an overnight starved rat was homogenized in 10-fold excess of ice-cold isolation buffer (10 mM Tris buffer adjusted to pH 7.4 with MOPS, 1 mM EGTA, 200 mM sucrose) using three to four strokes with a Teflon coated homogenizer operated at 1600 rpm. After centrifugation at 600 *g* at 4 °C for 10 min, the supernatant was recovered. Mitochondria were collected from the supernatant by centrifugation at 7000 *g* at 4 °C for 10 min and washed once in isolation buffer. For the

determination of succinate dehydrogenase activity in cell lines, cells were lysed in hypotonic phosphate buffer [20 mM KPi buffer pH 7.4] in three freeze-thaw cycles [29]. Protein concentration was determined using the bicinchoninic acid method (Thermo). Mitochondria were frozen down at high concentration (> 80 μg/ml) and adjusted to 5 μg/ml with isolation buffer on the day of the experiment.

Succinate dehydrogenase activity was determined using a published method [29]. Briefly, 10 μg of mitochondria were incubated at 37 °C in a mixture containing 25 mM potassium phosphate buffer pH 7.5, 1 $g.l^{-1}$ fatty acid free BSA, 300 μM KCN, 0.015 % DCPIP w/v (2,6-dichlorophenolindolphenol sodium salt dihydrate, Sigma) and the indicated concentrations of succinate and phosphoglycolate. The reaction was initiated by addition of 50 μM decylubiquinone (DUB, Santa-Cruz) and followed by reading the absorption at 600 nm. Incubation with 10 mM malonate in control samples was used to determine non-specific background activity.

Enolase activity was determined in a coupled reaction containing pyruvate kinase and lactate dehydrogenase in a reaction mixture containing 20 mM HEPES pH 7.5, 25 mM KCl, 1 mM DTT, 1 mM $MgCl_2$, 1 mM ADP, 150 μM NADH using rabbit muscle enolase (Sigma, 3.5 $mU.ml^{-1}$), lactate dehydrogenase (Roche, 0.7 U/ml) and pyruvate kinase (Roche, 1 U/ml) as coupling enzymes. The reaction was initiated in the presence of the indicated concentrations of phosphoglycolate by addition of the indicated concentrations of phosphoenolpyruvate and followed by reading the absorption at 340 nm.

Kinetic parameters were determined by curve fitting using the Prism 7 software package (GraphPad) and are presented as mean +/- s.e.m. of at least three independent determinations.

Alamar Blue

Cell proliferation was assessed using the Alamar Blue assay [30] essentially as described before [18]. Briefly, cells were plated in 96-well microtiter plates and cell viability was assessed 1 day and 4 days after plating by adding one-tenth volume of a 560-µM solution of resazurin (prepared in 0.9% NaCl solution from a 10-mM stock solution in DMSO), incubating for 4 h at 37 °C and measuring fluorescence upon excitation at 540 nm and emission at 590 nm. To correct for differences in plating efficiencies, we normalized the results obtained after 96 h to the results obtained after 24 h.

Western blot analysis

Cell lysates were prepared and western blots were performed using the same procedures as previously described [18]. Antibodies used were anti-PKM (Santa-Cruz, clone C-11, 1: 1000), anti-PGP (Santa-Cruz, clone E10, 1:1000), anti-β-actin (Sigma, clone AC-15, 1: 5000), anti-p53 (clone DO1, Santa-Cruz, 1:1000), anti-phospho p53 (Cell signalling, 1:1000), anti-P-H2AX (Millipore, 1:1000), anti-tubulin (Sigma, 1:40,000).

Analysis of metabolites by GC-MS

For metabolite analysis, cells were plated at 350,000 cells (HCT116), 125,000 cells (human fibroblasts) and 300,000 cells (U2OS) per well of a 6-well plate. The following day, medium was changed to DMEM medium without phenol red containing 3.6 $g.l^{-1}$ glucose, 10 % dialyzed foetal calf serum, 2 mM Ultraglutamine I (Lonza), and 100 $U.ml^{-1}$ Penicillin/Streptomycin (Lonza). Where indicated, phosphoglycolate was added at a concentration of 5 mM 5 h before harvesting. The extraction procedure of the intracellular metabolites, derivatization with MSTFA and methoxyamine, and GC/MS analysis were performed exactly as described in Collard, Baldin et al. [23]. Data were acquired in combined selected-ion monitoring and scanning mode (68–700 m/z). Compounds were identified on the basis of their retention time and characteristic ions (**Suppl. table 2**). Selected-ion monitoring (SIM) chromatograms of quantifyer ions were integrated using Masshunter software (Agilent), and areas were normalized to total ion current [31]. GC/MS experiments were performed three or four times on separate days over a time frame of six months. In each experiment, three tissue-culture wells were quenched, extracted and derivatized separately for each condition. Each sample was then analyzed separately (i.e., the samples were not pooled) by GC/MS. To facilitate the comparison between experiments performed on different days, values for each metabolite were normalized to the average of the values obtained in the untreated control cell line. In each experiment, the mean values for the normalized metabolite concentrations were calculated. The resulting three or four mean values (depending on the number of experiments) were then used to calculate means and s.e.m., which are presented in the figures. When multiple groups were compared, ANOVA was performed followed by a comparison of groups using Dunnett's test for multiple comparisons (when comparing to a single control group) or Tukey's test (when performing several pairwise comparisons). When the effects of PGP genotype and glycolate treatment were assessed, 2-way ANOVA was performed, followed by post-hoc tests corrected for multiple testing as described above. Absolute amounts of phosphoglycolate per mg of cellular protein were estimated by linear

regression of the peak areas extracted from SIM chromatograms from samples where known amounts of phosphoglycolate had been spiked in [18]. Absolute concentrations of phosphoglycolate were then estimated on the basis of a cellular water content of 4 µl per mg protein [32].

For figure 2A, isotopic distributions were corrected for the isotopic abundance using the known isotopic abundances of natural carbon and silicium with the Isocor package [33].

RESULTS

Mammalian cells can produce phosphoglycolate by phosphorylation of glycolate mainly via pyruvate kinase

To investigate the cellular origin of phosphoglycolate, we first needed to identify a suitable experimental system. We turned to cell lines where the enzyme phosphoglycolate phosphatase (PGP) had been genetically disabled. Previous work from our group has shown that this enzyme serves to eliminate two glycolytic side-products, 2-P-lactate and 4-P-erythronate [23]. In these studies, we did not observe any increase in baseline phosphoglycolate levels in PGP knockout cell lines above 5 μM. This indicated that either very little phosphoglycolate is produced in these cell lines or that phosphatases other than PGP dephosphorylate and eliminate it. Here, we measured phosphoglycolate concentrations in PGP knockout cell lines derived from the HCT116 colorectal cancer and U2OS osteosarcoma cell lines, which were cultured either in the presence or absence of glycolate, a potential biosynthetic precursor of glycolate. In untreated cells, no significant difference in phosphoglycolate and 3P-glycerol concentrations was observed between wild type and knockout cells (**Fig. 1A&B, Suppl. Fig. 2C and 3A,B&H**), whereas the other PGP substrates 4-P-erythronate and 2-P-lactate as well as 6P-gluconate were strongly increased in knockout cell lines (**Suppl. Fig 2 A,B&F, Suppl. Fig. 3C,E&F**). Overall, these observations were similar to what we had previously observed in HCT116 cells [18]. In contrast, when we challenged wild type and PGP knockout cell lines with 5 mM glycolate (i.e. a concentration in the range of those observed in patients with ethylene glycol intoxication [34]), we observed a strong increase in phosphoglycolate levels (**Fig. 1A&B, Suppl. Figure 3A&B**). Although glycolate concentrations were similar (Fig. 1B, Suppl. Fig. 3B), levels of phosphoglycolate in PGP knockout cell lines were consistently more than 5-fold higher than in wild type cells (**Fig. 1A, Suppl. Fig. 3A**) and strongly reduced when PGP was re-expressed (**Fig. 1A**), suggesting that PGP is the major enzyme responsible for the elimination of phosphoglycolate. Of note, while absolute concentrations of

phosphoglycolate reached more than 1 mM in glycolate-treated PGP knockout HCT116 cells (Fig. 1A), only a small reduction in viability was observed in these cell lines (**Suppl. Fig. 4**)

Phosphoglycolate could be formed either by direct phosphorylation of glycolate, or, possibly by a more complicated, as yet unknown, route involving its metabolism to glyoxylate. To distinguish between these possibilities, we treated cells with isotopically labelled glycolate carrying a deuterium on carbon 2. The only known metabolism of glycolate is indeed its conversion to glyoxylate, which leads to removal of one of the two hydrogens that are directly bound to C2. Thus, if phosphoglycolate were formed after metabolisation of glycolate to glyoxylate, we would expect a difference between the isotopomer distributions of phosphoglycolate and glycolate. In contrast, if phosphoglycolate were simply generated by phosphorylation of glycolate, we would expect similar isotopomer distributions for phosphoglycolate and glycolate. After treatment of cells, we extracted metabolites and analysed the mass isotopomer distributions of phosphoglycolate and glycolate by GC/MS. We observed that both were almost identical indicating that a kinase was likely responsible for the production of phosphoglycolate (**Fig. 2A**).

Pursuing the question of which kinase could be involved we focused on pyruvate kinase (PKM2) and glycerate kinase (GLYCTK), which act on substrates that resemble glycolate (**Fig. 2B**). Pyruvate kinase displays *in vitro* a side activity on glycolate that results in the formation of phosphoglycolate (and which is about 10-fold higher than the side activity observed with L-lactate) [35]. While such activity has not been described for GLYCTK, this enzyme transfers a phosphate group to the hydroxyl attached to the alpha carbon of glycerate, comparable to the position of the phosphate group in phosphoglycolate [36].

To assess the contribution of these enzymes to the formation of phosphoglycolate we transduced the HCT116 colorectal cancer cell line with lentiviral constructs driving the expression of shRNAs specific for PKM (coding for pyruvate kinase M1 and M2) or GLYCTK (coding for glycerate kinase). Quantitative RT-PCR analysis demonstrated a 40 % and 85 % decrease in transcript levels of GLYCTK and PKM, respectively (**Fig. 2C & D**), and western blot analysis showed an approximately 95 % downregulation of PKM protein in the cells expressing PKM shRNAs (not shown). Using GC/MS, we observed a 80 to 90 % decrease in phosphoglycolate and 2-P-lactate levels when PKM was downregulated, whereas these metabolites remained unchanged in cells in which GLYCTK gene was downregulated (**Fig. 2E&G**). Under these conditions, concentrations of the PGP substrate 4-P-erythronate were largely unaffected consistent with its production independent of pyruvate kinase. (**Fig.**

2F). Of note, these experiments were performed in the presence of pyruvate in the culture medium, to avoid major metabolic disturbances due to the knockdown of pyruvate kinase. Hence, lactate concentrations were not significantly reduced in PKM knockdown cells (**Fig. 2H**), excluding that the reduction of 2-P-lactate would be caused by a reduction of lactate rather than by the downregulation of pyruvate kinase.

Taken together, these results are consistent with the notion that the majority of phosphoglycolate and 2-P-lactate is produced by pyruvate kinase in this cell line. At this point we could not exclude that glycerate kinase contributes for the formation of phosphoglycolate since we were not able to reduce GLYCTK transcript levels by more than 50 %, despite attempting two different approaches (shRNA and lentiviral CRISPR/Cas9, data not shown). Given a more than 80 % reduction of phosphoglycolate in cell lines where pyruvate kinase was knocked down, the contribution of GLYCTK in our experimental system can only be minor.

In vivo, GLYCTK expression is largely limited to the liver and the small instestine (GTEX portal, [37]), whereas expression in most cell lines is much lower. Thus, it could be conceivable that in these organs GLYCTK plays a major role in the formation of phosphoglycolate. To test this possibility, we overexpressed mouse Glyctk cDNA in cell lines where pyruvate kinase had been knocked down. As shown in Figure 2I, Glyctk mRNA levels upon overexpression were comparable to the ones observed in mouse liver. This led to a small increase in phosphoglycolate concentrations (**Fig. 2J**), which represented less than 10 % of the reduction that had been observed upon pyruvate kinase knockdown, consistent with the notion that GLYCTK can indeed contribute to a small extent to the production of phosphoglycolate.

Of note, one might ask the question whether phosphoglycerate kinase might also be involved the production of phosphoglycolate. At first sight this seemed very unlikely, since this kinase in its normal reaction phosphorylates the carboxylic function rather than a hydroxyl group. Nevertheless, we tested whether shRNA-mediated knockdown of PGK1 (the dominant form of PGK in the HCT116 cell line) might affect phosphoglycolate production. Introduction of two different shRNAs led to an 80 - 90 % downregulation of PGK1 mRNA levels (**Suppl. Fig. 5A**). A concomitant increase of the ratio of triose phosphates to 3-phosphoglycerate concentrations indicated that the combined action of GAPDH and PGK1 was indeed inhibited (**Suppl. Fig. 5B**). Yet, this did not lead to any reduction of cellular phosphoglycolate levels (**Suppl. Fig. 5C**).

Taken together, we conclude that phosphoglycolate in HCT116 cells is mainly formed by the action of pyruvate kinase on glycolate.

Accumulation of phosphoglycolate indirectly leads to an inhibition of phosphoglycerate mutase

Phosphoglycerate mutases (PGAMs) serve to interconvert 2-P-glycerate and 3-P-glycerate (**Fig. 3A**). To catalyse this reaction, mammalian PGAMs need to be phosphorylated on a catalytic histidine residue in a reaction that uses 2,3-bisphosphoglycerate or (less-efficiently) 1,3-bisphosphoglycerate (so-called priming-phosphorylation) (**Fig. 3B**) [38]. Under normal conditions, substrate binding leads to the formation of a 2,3-bisphosphoglycerate reaction intermediate and the release of either 2-P-glycerate or 3-P-glycerate, as well as a restoration of the enzyme-bound phosphate group. Of note, phosphoglycolate can also bind to mammalian PGAMs [39]. Yet, this does not lead to a 2,3-bisphosphoglycerate reaction intermediate, but rather to the hydrolysis of the phosphate group bound to the enzyme, thereby preventing the enzyme from performing its normal function [12]. Before the enzyme can work again, it therefore needs to be primed again.

To test whether phosphoglycolate concentrations in cells suffice to affect PGAM activity, we measured the ratio of 3-P-glycerate and 2-P-glycerate concentrations in PGP wild type and knockout HCT116 cells (**Fig. 3C, Suppl. Fig. 6A&B)**. This ratio increased more than 2-fold when we added glycolate to PGP knockout cells, but remained unchanged in wild type cells (**Fig. 3C**). This increase was abolished upon re-expression of PGP (**Suppl. Fig. 2F**). It was also observed in the PGP deficient U2OS cells and, to a lower degree, in wild type cells treated with glycolate (**Suppl. Fig. 7A-C**) These observations were consistent with the hypothesis that high concentrations of phosphoglycolate observed in PGP knockout cells suffice to block PGAM activity by making it dependent on continuous re-priming. To test this hypothesis, we overexpressed gpmI, a 2,3-bisphosphoglycerate-independent phosphoglycerate mutase from *E. coli*. This enzyme does not require priming phosphorylation [40] and therefore should not be affected by the presence of phosphoglycolate. Indeed, when we treated PGP knockout cell lines overexpressing gpmI with glycolate, the increase in the ratio of 3-P-glycerate to 2-P-glycerate was significantly blunted (**Fig. 3C**) whereas phosphoglycolate levels were unchanged (**Fig. 3D**).

Surprisingly, PGP knockout cells incubated with glycolate showed lower phosphoenolpyruvate (PEP) concentrations and a 2-fold increase in the ratio of 2-phosphoglycerate to PEP (**Suppl. Fig. 6D & E**). In glycolysis, the reaction from 2-

phosphoglycerate to PEP is catalyzed by the enzyme enolase (Fig. 3A). Our data therefore suggested that enolase might be inhibited by phosphoglycolate. Indeed, purified enolase was inhibited by 2-P-glycolate with a Ki of approximately 160 μM (**Suppl. Fig. 6F**).

Metabolite changes are consistent with an inhibition of triose phosphate isomerase by phosphoglycolate in glycolate-treated PGP knockout cells

Phosphoglycolate is a well-known inhibitor (Ki ≈ 20 μM) of the enzyme triose phosphate isomerase due to its similarity to a transition state occurring during the catalytic cycle of this enzyme [8-10]. If phosphoglycolate inhibits triose phosphate isomerase in cells we expect to observe an increase in the ratio of dihydroxyacetone-P (DHAP, the substrate) to glyceraldehyde 3-P (GAP, the product) (see Fig. 3A for schematic). Unfortunately, we were unable to assess glyceraldehyde 3-P levels reliably and therefore we cannot report this ratio. We did observe a substantial increase in the concentration of DHAP when glycolate was added to PGP knockout cells (**Suppl. Fig. 2D, 3G and 6C**). This is consistent with the idea that phosphoglycolate accumulation indeed exerts an inhibition on triose-phosphate isomerase in our experimental model. Yet, this conclusion has to be taken with caution since the increase of DHAP could also be caused by a build-up of metabolites upstream of phosphoglycerate mutase, which is inhibited by phosphoglycolate. The combined action of triose phosphate isomerase, glyceraldehyde-3-phosphate dehydrogenase and phosphoglycerate kinase is commonly assumed to be quite close to equilibrium [41]. Hence, the observed increases in 3-P-glycerate levels (**Suppl. Fig. 2E, 6A & 7B**) are expected to lead to increases in upstream metabolites, including DHAP, even if triose phosphate isomerase is not inhibited. In the absence of a method that allows us to quantify glyceraldehyde-3-P and 1,3-bisphosphoglycerate, we cannot clearly distinguish between these two possibilities.

Of note, the analysis of triose phosphate activity in cellular lysates would not help us clarify this issue, since the dilution of cellular lysates in the assay also dilutes the competitive inhibitor phosphoglycolate. Extrapolations to the situation in cells would therefore be difficult, in particular if these measurements are performed with saturating substrate concentrations.

Phosphoglycolate is a very efficient inhibitor of succinate dehydrogenase

When looking at the change in the concentrations of other metabolites we noticed that the addition of glycolate to PGP knockout cells caused a marked increase in the concentration of succinate (**Fig. 4A**), while it caused a decrease in the concentration of downstream

metabolites in the Krebs cycle (fumarate and malate - **Fig. 4B & C**). We also noted that aspartate, which is formed by transamination of oxaloacetate, was also markedly decreased (**Fig. 4D&E**). These data suggested an inhibition of succinate dehydrogenase by phosphoglycolate, most likely of the competitive type since phosphoglycolate is a structural analogue of succinate (**Fig. 4F**). This was indeed confirmed by *in vitro* measurement of succinate dehydrogenase activity in rat liver mitochondria; a competitive inhibition with a Ki of 7.4 μM was observed (**Fig. 4G**). Of note, succinate deydrogenase activity in lysates from PGP wild type and knockout cell lines was virtually identical (**Suppl. Fig. 8A**) and inhibited by the addition of phosphoglycolate to a similar degree as in rat liver mitochondria (**Suppl. Fig. 8B**). This is consistent with the idea that the inhibition of succinate dehydrogenase by phosphoglycolate is responsible for the metabolite changes. At this point it is unclear how phosphoglycolate enters the mitochondria, but, given the size and charge distribution of phosphoglycolate, the α-ketoglutarate/malate antiporter might be a candidate [42].

Phosphoglycolate concentrations released during DNA damage repair are not sufficient to elicit metabolic changes in cancer cell lines.

It has been recently reported that PGP knockout mice die during embryogenesis [15]. Embryonic fibroblasts obtained from PGP knockout embryos grow much slower than their wild type counterparts under normoxia, but grow normally under hypoxia. This profound oxygen-dependent growth inhibition has been attributed to the accumulation of oxidative DNA damage lesions, which can lead to the formation of phosphoglycolate [15]. Yet, it was unclear whether the phosphoglycolate produced from the repair of 3' phosphoglycolate ends (**Suppl. Fig. 1A**) would be sufficient to modulate cellular phosphoglycolate concentrations to a relevant extent.

To test this, we treated PGP knockout lines obtained from the HCT116 colorectal carcinoma and U2OS osteosarcoma cell line with Bleomycin, the chemotherapeutic agent that is best characterized to lead to the production of phosphoglycolate [43], and with ionizing radiation (**Fig. 5**). Cells indeed underwent considerable DNA damage as documented by the western blots for DNA damage response pathway components p53, phospho-p53 and phospho-H2AX (**Fig. 5D,H&L**). Phosphoglycolate levels as well as surrogate markers indicative of an inhibition of succinate dehydrogenase or PGAM were assessed by GC/MS. Yet, we did not observe any significant increase of phosphoglycolate upon treatment with

Bleomycin or irradiation (**Fig. 5A,E&I**). Likewise, we did not observe any change in succinate or 3PG/2PG ratios indicating that no inhibition of succinate dehydrogenase or phosphoglycerate mutases had occurred (**Fig. 5B,C,F,G,J&K**). This demonstrates that phosphoglycolate production during DNA damage repair is too small to lead to major metabolic changes in our experimental systems.

DISCUSSION

Phosphoglycolate is a common metabolite in photosynthetic plants, where it is formed when Rubisco erroneously uses O_2 instead of CO_2 as a substrate [44]. In contrast, in mammals phosphoglycolate is not part of any known metabolic pathway. In the present study, we elucidated the formation and biological effects of phosphoglycolate in mammalian cell lines.

At baseline, phosphoglycolate levels were < 5 μM in both wild type and PGP knockout cell lines. In contrast, we observed a strong increase when cells were treated with exogenous glycolate. This increase was more than 5-fold stronger in PGP knockout cell lines consistent with the idea that PGP is the main enzyme responsible for the degradation of this metabolite. Using isotopically labeled glycolate, we demonstrated that phosphoglycolate was mainly synthesized by direct phosphorylation. Two kinases are known to potentially phosphorylate a hydroxyl group present on carbon 2 of a carboxylic acid. One is pyruvate kinase, which is known to display side activities that lead to the phosphorylation of lactate and glycolate [45]. Another one is glycerate kinase, which converts glycerate to 2-P-glycerate in vertebrates and in bacteria [46]. Knockdown of pyruvate kinase M1/2 led to a more than 80 % decrease in the formation of phosphoglycolate in PGP deficient cells, while this was not the case if the glycerate kinase gene was inactivated. These findings indicate that the side activity of pyruvate kinase is responsible for the formation of phosphoglycolate.

Two additional observations are important in these experiments. First of all, we also demonstrated that another PGP substrate, 2-P-lactate, is also produced in a pyruvate kinase dependent manner (whereas the PGP substrate 4-P-erythronate is largely unaffected). This means that PGP in fact eliminates two side products of pyruvate kinase, phosphoglycolate and 2-P-lactate, and a side product of glyceraldehyde 3-phosphate dehydrogenase, 4-P-erythronate [18]. It is remarkable that its rather broad substrate spectrum (i.e. a certain lack of specificity) allows PGP to make up for the errors committed by two major glycolytic enzymes. Secondly, treatment of cells with 5 mM glycolate at first sight seems like something extremely non-physiological. Yet, it should be noted that intoxications with ethylene glycol commonly lead to similar concentrations in blood [34]. As such, the metabolic changes observed in glycolate-treated PGP knockout cells indeed represent the situation that cells would encounter during ethylene glycol intoxication in the absence of PGP. Obviously, this situation is exceedingly rare, and there need to be other reasons why PGP has retained its activity towards phosphoglycolate during evolution. One explanation would be that the requirement to

maintain activity on both 2-P-lactate and 4-P-erythronate inevitably leads to some activity on phosphoglycolate. Retaining the activity towards phosphoglycolate, which is almost absent in cells, might simply not have been a disadvantage. Of course, it is also conceivable that the dephosphorylation of phosphoglycolate might have represented a significant selective advantage at some point during evolution. For example, inactivation of the yeast homolog of PGP, pho13, leads to significant increases in phosphoglycolate levels [18]. At this point it is unclear why this would represent a selective advantage. Yet, we did not further pursue this since preliminary experiments indicated that phosphoglycolate production in yeast might be more complex that in mammals (data not shown).

In the absence of glycolate addition, the level of phosphoglycolate is below 5 μM, even in cells that are PGP-deficient. This is most likely due to the fact that glycolate levels are very low. In mammalian cells, glycolate essentially results from the reduction of glyoxylate by hydroxypyruvate/glyoxylate reductase, an enzyme present in the cytosol and in mitochondria [47]. This reaction prevents glyoxylate from being irreversibly converted to oxalate by lactate dehydrogenase in the cytoplasm [47, 48]. Glycolate is converted back to glyoxylate and eventually glycine in the peroxisomes thanks to the action of glycolate oxidase (L-2-hydroxyacid oxidase I) and alanine glyoxylate aminotransferase (AGT) [49, 50]. This system appears to be very efficient in the cell models that we used, and thereby prevents the formation of phosphoglycolate.

These observations left open the possibility that DNA damage could be a relevant source of phosphoglycolate, which could lead to metabolic effects with an important role in the cellular DNA damage response. To test this, we first investigated secondary metabolic changes under conditions where phosphoglycolate concentrations were moderately (i.e. glycolate-treated wild type cells) or highly (i.e. glycolate-treated PGP knockout cells) elevated. We observed that high concentrations of phosphoglycolate lead to profound metabolic disturbances. Some of these changes were expected based on the literature. Yet, others (such as the inhibition of succinate dehydrogenase) are described here for the first time.

On the one hand, we observed metabolite changes that are consistent with an inhibition of phosphoglycerate mutase (**Suppl. Fig. 1C**). This result was expected, since phosphoglycolate is well known to cause the dephosphorylation of a catalytic histidine residue in phosphoglycerate mutases [39]. To be able to act, phosphoglycerate mutases then need to be phosphorylated by 2,3-bisphosphoglycerate (or less efficiently 1,3-bisphosphoglycerate) (**Fig. 3B**). In line with this model, we were able to prevent the inhibition

of the phosphoglycerate mutase step by expressing a bacterial phosphoglycerate mutase enzyme that does not use a phosphohistidine intermediate [46] (**Fig. 3C**).

On the other hand, we made the surprising observation that very high concentrations of phosphoglycolate were associated with a strong increase in succinate concentrations (**Fig. 4A**). *In vitro* studies using purified mitochondrial extracts subsequently allowed us to establish that phosphoglycolate competitively inhibits succinate dehydrogenase with a Ki of <10μM. This competition is likely a consequence of a certain structural similarity and similar charge distribution between 2-P-glycolate and succinate (**Fig. 4F**).

These striking metabolic changes were observed when we treated PGP knockout cell lines with glycolate, which led to very high levels of phosphoglycolate. In contrast, secondary effects were almost absent when we treated wild type cells with glycolate, even though this led to clear increases in phosphoglycolate levels reaching more than 40 μM. With regard to the changes of glycolytic intermediates, this is not surprising, since the enzymes inhibited by phosphoglycolate (TPI, PGAM and enolase) are commonly believed to act close to equilibrium and have a large reserve capacity [41]. Thus, inhibition of these enzymes is not necessarily expected to lead to changes in metabolite concentrations. In fact, even a strong change in the ratio of substrate to product concentrations should not be taken as an indication that glycolytic flux is changed. Yet, this does not mean that inhibition of these enzymes is always irrelevant. For examples, inhibition of PGAM activity and the resulting increase in 3P-glycerate concentrations can lead to an increase in serine synthesis [38, 51]. With regard to the inhibition of succinate dehydrogenase, we also need to take into account that phosphoglycolate first needs to be taken up in the mitochondria and that effective concentrations there might be significantly lower than in the cytoplasm.

We reasoned that DNA-damage-induced phosphoglycolate release could only lead to secondary metabolic changes, if it actually increased cellular phosphoglycolate concentrations To test this, we treated PGP knockout cells with Bleomycin, the prototypical chemotherapeutic drug that is known to lead to phosphoglycolate release, and with ionizing radiation. In two different cell lines (HCT116 and U2OS), we did not find any significant increase in Bleomycin-treated or irradiated PGP-deficient cells. This indicated that it is extremely unlikely that phosphoglycolate released during DNA-damage could directly contribute to secondary metabolic changes in our experimental systems.

The overall number of oxidative hits in human fibroblasts has been estimated to be between 9000 and 31500 per day [52, 53] and the majority lead to the formation of 8-oxoguanine. Even if we make the unrealistic assumption that all lesions would result in

phosphoglycolate release and if we consider very small cell types like mouse lymphocytes with a cellular volume of 120 femtoliters [54], this only amounts to an increase of 0.4 μmol/l per day, which, in one day, would lead to a concentration that is at least 10-fold lower than the Ki for any of the known inhibitory effects of phosphoglycolate. Thus, it is unlikely that under normoxic conditions, proliferating cell types can accumulate sufficient phosphoglycolate to account for measurable metabolic effects.

Yet, it has previously been suggested that DNA-damage-dependent phosphoglycolate played a role in the growth-defect in PGP knockout MEFs [15]. Segerer and colleagues observed that these cells grow dramatically slower than their wild type counterpart. Interestingly, this difference was abolished when these cells were cultured under hypoxic conditions or when they were treated with an inhibitor of TDP1 [19], one of the enzymes that is responsible for the repair of 3'-phosphoglycolate ends (Suppl. Fig. 1A). At first sight, this might suggest that oxygen-dependent phosphoglycolate release might play a role in the growth deficit of MEFs. Yet, this conclusion is incorrect, since TDP1 removes glycolate and not phosphoglycolate from DNA ends [5-7] (see schematic in Suppl. Fig. 1A). Therefore, inhibition of TDP1 is not expected to decrease phosphoglycolate concentrations, but might rather increase phosphoglycolate formation since remaining 3'-phosphoglycolate-DNA ends could be repaired by the enzyme APE1 (which actually leads to a release of phosphoglycolate)[3]. Thus, the observation that treatment with a TDP1 inhibitor rescues growth of PGP mutant MEFs, does not allow any conclusion on the involvement of phosphoglycolate in this process, but rather indicates that the cause for the growth inhibition in PGP mutant MEFs is likely more complex than previously assumed.

Of note, we do not encounter a major reduction in viability when we genetically inactivate PGP in human normal fibroblasts (**Suppl. Fig. 9**). Comparable to our observations in cancer cell lines, human fibroblasts with complete PGP knockout show 25-fold, 9-fold and 110-fold increases in 2P-lactate, 4-P-erythronate and 6P-gluconate, respectively (**Suppl. Fig. 9B,C&F**), whereas phosphoglycolate and 3P-glycerol levels remain unchanged or are reduced (**Suppl. Fig. 9D&E**). This suggests that the difference in behaviour in MEFs is not just a question of being "normal" versus being "cancerous". MEFs are known to be exquisitely sensitive to oxidative stress and show more oxidative DNA damage than their human counterparts [55]. Thus it might be conceivable that MEFs for unknown reasons show extraordinarily high oxygen-dependent phosphoglycolate release or changes in 3P-glycerol metabolism. Alternatively, PGP knockout MEFs might simply not be able to maintain sufficient NADPH synthesis and anti-oxidative defense, if 4P-erythronate accumulates and

inhibits 6-P-gluconate dehydrogenase activity similar to the situation in other PGP knockout cells (see **Suppl. Fig. 1B, 3F, 9F**). Future experiments in MEFs will have to resolve these questions.

The situation might be quite different when cells are treated with Bleomycin or ionizing radiation, since in cell-free conditions these treatments can lead to very high concentrations of 3'phosphoglycolate ends [56]. Yet, in our experiments we did not observe any significant increase of phosphoglycolate concentrations upon DNA damage in two different cell lines, although several different concentrations and time-points were assessed. This indicates that in HCT116 and U2OS cells, phosphoglycolate does not play a role in a metabolic response to DNA damage.

ACKNOWLEDGEMENTS & FUNDING INFORMATION:
The authors are grateful for funding obtained from WELBIO (to EVS), Fondation Contre Le Cancer (EVS and GTB), Mandat d'impulsion – FNRS (GTB), FRIA-FNRS (FB), PDR-FNRS (EVS), European Research Council (GTB) and the Fonds Joseph Maisin. We thank Anabelle Decottignies (UCLouvain, Brussels, Belgium) for sharing cell lines, Feng Zhang (MIT, Cambridge, MA, USA) for the CRISPR/Cas9 vector and Lawrence Povirk (University of Richmond, Virginia, USA) for guidance on the TDP1 function.

DECLARATIONS OF INTEREST:
The authors do not have any conflict of interest to declare.

AUTHOR CONTRIBUTION STATEMENT
IG, FB, MB, JG performed experiments, IG, FB, MB, EVS, GTB planned experiments and analyzed data. The paper was written by IG, FB, EVS and GTB. All authors approved the final version.

References:

1 Henner, W. D., Rodriguez, L. O., Hecht, S. M. and Haseltine, W. A. (1983) gamma Ray induced deoxyribonucleic acid strand breaks. 3' Glycolate termini. J Biol Chem. **258**, 711-713

2 Fung, H. and Demple, B. (2011) Distinct roles of Ape1 protein in the repair of DNA damage induced by ionizing radiation or bleomycin. J Biol Chem. **286**, 4968-4977

3 Parsons, J. L., Dianova, II and Dianov, G. L. (2004) APE1 is the major 3'-phosphoglycolate activity in human cell extracts. Nucleic acids research. **32**, 3531-3536

4 Xu, Y. J., Kim, E. Y. and Demple, B. (1998) Excision of C-4'-oxidized deoxyribose lesions from double-stranded DNA by human apurinic/apyrimidinic endonuclease (Ape1 protein) and DNA polymerase beta. J Biol Chem. **273**, 28837-28844

5 Zhou, T., Akopiants, K., Mohapatra, S., Lin, P. S., Valerie, K., Ramsden, D. A., Lees-Miller, S. P. and Povirk, L. F. (2009) Tyrosyl-DNA phosphodiesterase and the repair of 3'-phosphoglycolate-terminated DNA double-strand breaks. DNA Repair (Amst). **8**, 901-911

6 Zhou, T., Lee, J. W., Tatavarthi, H., Lupski, J. R., Valerie, K. and Povirk, L. F. (2005) Deficiency in 3'-phosphoglycolate processing in human cells with a hereditary mutation in tyrosyl-DNA phosphodiesterase (TDP1). Nucleic acids research. **33**, 289-297

7 Inamdar, K. V., Pouliot, J. J., Zhou, T., Lees-Miller, S. P., Rasouli-Nia, A. and Povirk, L. F. (2002) Conversion of phosphoglycolate to phosphate termini on 3' overhangs of DNA double strand breaks by the human tyrosyl-DNA phosphodiesterase hTdp1. J Biol Chem. **277**, 27162-27168

8 Go, M. K., Koudelka, A., Amyes, T. L. and Richard, J. P. (2010) Role of Lys-12 in catalysis by triosephosphate isomerase: a two-part substrate approach. Biochemistry. **49**, 5377-5389

9 Zhai, X., Amyes, T. L., Wierenga, R. K., Loria, J. P. and Richard, J. P. (2013) Structural mutations that probe the interactions between the catalytic and dianion activation sites of triosephosphate isomerase. Biochemistry. **52**, 5928-5940

10 Zhai, X., Reinhardt, C. J., Malabanan, M. M., Amyes, T. L. and Richard, J. P. (2018) Enzyme Architecture: Amino Acid Side-Chains That Function To Optimize the Basicity of the Active Site Glutamate of Triosephosphate Isomerase. J Am Chem Soc. **140**, 8277-8286

11 Rose, Z. B. and Liebowitz, J. (1970) 2,3-diphosphoglycerate phosphatase from human erythrocytes. General properties and activation by anions. J Biol Chem. **245**, 3232-3241

12 Rose, Z. B. and Dube, S. (1978) Phosphoglycerate mutase. Kinetics and effects of salts on the mutase and bisphosphoglycerate phosphatase activities of the enzyme from chicken breast muscle. J Biol Chem. **253**, 8583-8592

13 Maddocks, O. D. and Vousden, K. H. (2011) Metabolic regulation by p53. Journal of molecular medicine. **89**, 237-245

14 Berkers, C. R., Maddocks, O. D., Cheung, E. C., Mor, I. and Vousden, K. H. (2013) Metabolic regulation by p53 family members. Cell Metab. **18**, 617-633

15 Segerer, G., Hadamek, K., Zundler, M., Fekete, A., Seifried, A., Mueller, M. J., Koentgen, F., Gessler, M., Jeanclos, E. and Gohla, A. (2016) An essential developmental function for murine phosphoglycolate phosphatase in safeguarding cell proliferation. Scientific reports. **6**, 35160

16 Seifried, A., Bergeron, A., Boivin, B. and Gohla, A. (2016) Reversible oxidation controls the activity and oligomeric state of the mammalian phosphoglycolate phosphatase AUM. Free radical biology & medicine. **97**, 75-84

17 Badwey, J. A. (1977) Phosphoglycolate phosphatase in human erythrocytes. J Biol Chem. **252**, 2441-2443
18 Collard, F., Baldin, F., Gerin, I., Bolsee, J., Noel, G., Graff, J., Veiga-da-Cunha, M., Stroobant, V., Vertommen, D., Houddane, A., Rider, M. H., Linster, C. L., Van Schaftingen, E. and Bommer, G. T. (2016) A conserved phosphatase destroys toxic glycolytic side products in mammals and yeast. Nature chemical biology. **12**, 601-607
19 Segerer, G., Engelmann, D., Kaestner, A., Trotzmuller, M., Kofeler, H., Stigloher, C., Thiele, C., Jeanclos, E. and Gohla, A. (2018) A phosphoglycolate phosphatase/AUM-dependent link between triacylglycerol turnover and epidermal growth factor signaling. Biochimica et biophysica acta. **1863**, 584-594
20 Mugabo, Y., Zhao, S., Seifried, A., Gezzar, S., Al-Mass, A., Zhang, D., Lamontagne, J., Attane, C., Poursharifi, P., Iglesias, J., Joly, E., Peyot, M. L., Gohla, A., Madiraju, S. R. and Prentki, M. (2016) Identification of a mammalian glycerol-3-phosphate phosphatase: Role in metabolism and signaling in pancreatic beta-cells and hepatocytes. Proceedings of the National Academy of Sciences of the United States of America
21 Gerin, I., Ury, B., Breloy, I., Bouchet-Seraphin, C., Bolsee, J., Halbout, M., Graff, J., Vertommen, D., Muccioli, G. G., Seta, N., Cuisset, J. M., Dabaj, I., Quijano-Roy, S., Grahn, A., Van Schaftingen, E. and Bommer, G. T. (2016) ISPD produces CDP-ribitol used by FKTN and FKRP to transfer ribitol phosphate onto alpha-dystroglycan. Nat Commun. **7**, 11534
22 Fellmann, C., Hoffmann, T., Sridhar, V., Hopfgartner, B., Muhar, M., Roth, M., Lai, D. Y., Barbosa, I. A., Kwon, J. S., Guan, Y., Sinha, N. and Zuber, J. (2013) An optimized microRNA backbone for effective single-copy RNAi. Cell reports. **5**, 1704-1713
23 Collard, F., Baldin, F., Gerin, I., Bolsee, J., Noel, G., Graff, J., Veiga-da-Cunha, M., Stroobant, V., Vertommen, D., Houddane, A., Rider, M. H., Linster, C. L., Van Schaftingen, E. and Bommer, G. T. (2016) A conserved phosphatase destroys toxic glycolytic side products in mammals and yeast. Nat Chem Biol. **12**, 601-607
24 Mattiussi, M., Tilman, G., Lenglez, S. and Decottignies, A. (2012) Human telomerase represses ROS-dependent cellular responses to Tumor Necrosis Factor-alpha without affecting NF-kappaB activation. Cellular signalling. **24**, 708-717
25 Sanjana, N. E., Shalem, O. and Zhang, F. (2014) Improved vectors and genome-wide libraries for CRISPR screening. Nat Methods. **11**, 783-784
26 Gerin, I., Noel, G., Bolsee, J., Haumont, O., Van Schaftingen, E. and Bommer, G. T. (2014) Identification of TP53-induced glycolysis and apoptosis regulator (TIGAR) as the phosphoglycolate-independent 2,3-bisphosphoglycerate phosphatase. Biochem J. **458**, 439-448
27 Jordan, M., Schallhorn, A. and Wurm, F. M. (1996) Transfecting mammalian cells: optimization of critical parameters affecting calcium-phosphate precipitate formation. Nucleic acids research. **24**, 596-601
28 Frezza, C., Cipolat, S. and Scorrano, L. (2007) Organelle isolation: functional mitochondria from mouse liver, muscle and cultured fibroblasts. Nature protocols. **2**, 287-295
29 Spinazzi, M., Casarin, A., Pertegato, V., Salviati, L. and Angelini, C. (2012) Assessment of mitochondrial respiratory chain enzymatic activities on tissues and cultured cells. Nature protocols. **7**, 1235-1246
30 O'Brien, J., Wilson, I., Orton, T. and Pognan, F. (2000) Investigation of the Alamar Blue (resazurin) fluorescent dye for the assessment of mammalian cell cytotoxicity. Eur J Biochem. **267**, 5421-5426
31 Jaeger, C., Glaab, E., Michelucci, A., Binz, T. M., Koeglsberger, S., Garcia, P., Trezzi, J. P., Ghelfi, J., Balling, R. and Buttini, M. (2015) The mouse brain metabolome: region-

specific signatures and response to excitotoxic neuronal injury. Am J Pathol. **185**, 1699-1712
32 Feijo Delgado, F., Cermak, N., Hecht, V. C., Son, S., Li, Y., Knudsen, S. M., Olcum, S., Higgins, J. M., Chen, J., Grover, W. H. and Manalis, S. R. (2013) Intracellular water exchange for measuring the dry mass, water mass and changes in chemical composition of living cells. PLoS One. **8**, e67590
33 Millard, P., Letisse, F., Sokol, S. and Portais, J. C. (2012) IsoCor: correcting MS data in isotope labeling experiments. Bioinformatics. **28**, 1294-1296
34 Rosano, T. G., Swift, T. A., Kranick, C. J. and Sikirica, M. (2009) Ethylene glycol and glycolic acid in postmortem blood from fatal poisonings. J Anal Toxicol. **33**, 508-513
35 Kayne, F. J. (1974) Pyruvate kinase catalyzed phosphorylation of glycolate. Biochem Biophys Res Commun. **59**, 8-13
36 Katayama, H., Kitagawa, Y. and Sugimoto, E. (1980) Purification of rat liver glycerate kinase and studies of its enzymatic and immunological properties. J Biochem. **88**, 765-773
37 Gamazon, E. R., Segre, A. V., van de Bunt, M., Wen, X., Xi, H. S., Hormozdiari, F., Ongen, H., Konkashbaev, A., Derks, E. M., Aguet, F., Quan, J., Consortium, G. T., Nicolae, D. L., Eskin, E., Kellis, M., Getz, G., McCarthy, M. I., Dermitzakis, E. T., Cox, N. J. and Ardlie, K. G. (2018) Using an atlas of gene regulation across 44 human tissues to inform complex disease- and trait-associated variation. Nature genetics. **50**, 956-967
38 Oslund, R. C., Su, X., Haugbro, M., Kee, J. M., Esposito, M., David, Y., Wang, B., Ge, E., Perlman, D. H., Kang, Y., Muir, T. W. and Rabinowitz, J. D. (2017) Bisphosphoglycerate mutase controls serine pathway flux via 3-phosphoglycerate. Nature chemical biology. **13**, 1081-1087
39 Fothergill-Gilmore, L. A. and Watson, H. C. (1989) The phosphoglycerate mutases. Adv Enzymol Relat Areas Mol Biol. **62**, 227-313
40 Collet, J. F., Stroobant, V. and Van Schaftingen, E. (2001) The 2,3-bisphosphoglycerate-independent phosphoglycerate mutase from Trypanosoma brucei: metal-ion dependency and phosphoenzyme formation. FEMS Microbiol Lett. **204**, 39-44
41 Voet, D. and Voet, J. G. (2011) Biochemistry. John Wiley & Sons, Hoboken, NJ
42 Palmieri, F. (2013) The mitochondrial transporter family SLC25: identification, properties and physiopathology. Mol Aspects Med. **34**, 465-484
43 Giloni, L., Takeshita, M., Johnson, F., Iden, C. and Grollman, A. P. (1981) Bleomycin-induced strand-scission of DNA. Mechanism of deoxyribose cleavage. J Biol Chem. **256**, 8608-8615
44 Erb, T. J. and Zarzycki, J. (2018) A short history of RubisCO: the rise and fall (?) of Nature's predominant CO2 fixing enzyme. Current opinion in biotechnology. **49**, 100-107
45 Ash, D. E., Goodhart, P. J. and Reed, G. H. (1984) ATP-dependent phosphorylation of alpha-substituted carboxylic acids catalyzed by pyruvate kinase. Archives of biochemistry and biophysics. **228**, 31-40
46 Fraser, H. I., Kvaratskhelia, M. and White, M. F. (1999) The two analogous phosphoglycerate mutases of Escherichia coli. FEBS letters. **455**, 344-348
47 Cramer, S. D., Ferree, P. M., Lin, K., Milliner, D. S. and Holmes, R. P. (1999) The gene encoding hydroxypyruvate reductase (GRHPR) is mutated in patients with primary hyperoxaluria type II. Human molecular genetics. **8**, 2063-2069
48 Banner, M. R. and Rosalki, S. B. (1967) Glyoxylate as a substrate for lactate dehydrogenase. Nature. **213**, 726-727

49 Baker, P. R., Cramer, S. D., Kennedy, M., Assimos, D. G. and Holmes, R. P. (2004) Glycolate and glyoxylate metabolism in HepG2 cells. Am J Physiol Cell Physiol. **287**, C1359-1365
50 Holmes, R. P. and Assimos, D. G. (1998) Glyoxylate synthesis, and its modulation and influence on oxalate synthesis. J Urol. **160**, 1617-1624
51 Madhukar, N. S., Warmoes, M. O. and Locasale, J. W. (2015) Organization of enzyme concentration across the metabolic network in cancer cells. PLoS One. **10**, e0117131
52 Helbock, H. J., Beckman, K. B., Shigenaga, M. K., Walter, P. B., Woodall, A. A., Yeo, H. C. and Ames, B. N. (1998) DNA oxidation matters: the HPLC-electrochemical detection assay of 8-oxo-deoxyguanosine and 8-oxo-guanine. Proceedings of the National Academy of Sciences of the United States of America. **95**, 288-293
53 Chen, Q., Fischer, A., Reagan, J. D., Yan, L. J. and Ames, B. N. (1995) Oxidative DNA damage and senescence of human diploid fibroblast cells. Proceedings of the National Academy of Sciences of the United States of America. **92**, 4337-4341
54 Milo, R., Jorgensen, P., Moran, U., Weber, G. and Springer, M. (2010) BioNumbers--the database of key numbers in molecular and cell biology. Nucleic acids research. **38**, D750-753
55 Parrinello, S., Samper, E., Krtolica, A., Goldstein, J., Melov, S. and Campisi, J. (2003) Oxygen sensitivity severely limits the replicative lifespan of murine fibroblasts. Nature cell biology. **5**, 741-747
56 Chen, B., Zhou, X., Taghizadeh, K., Chen, J., Stubbe, J. and Dedon, P. C. (2007) GC/MS methods to quantify the 2-deoxypentos-4-ulose and 3'-phosphoglycolate pathways of 4' oxidation of 2-deoxyribose in DNA: application to DNA damage produced by gamma radiation and bleomycin. Chem Res Toxicol. **20**, 1701-1708

FIGURES:

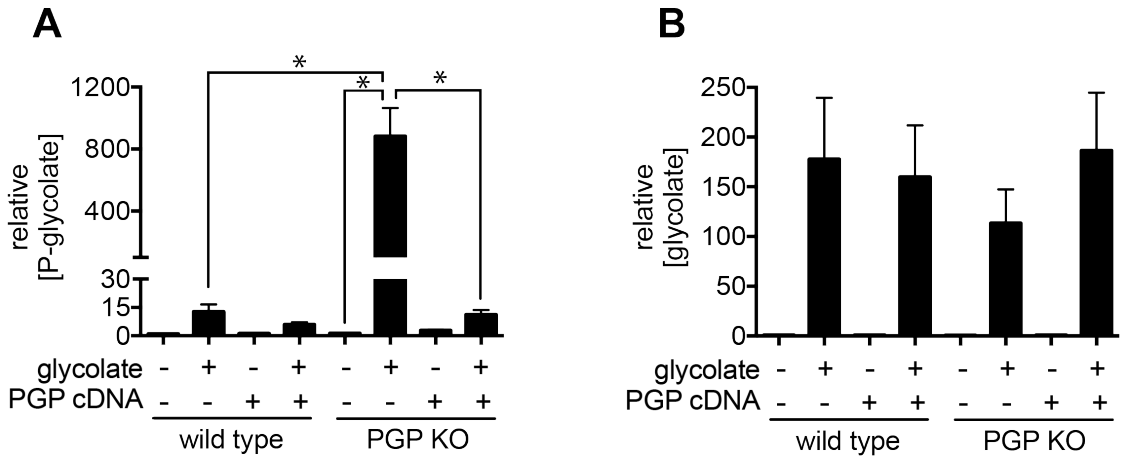

Figure 1. Glycolate supplementation leads to accumulation of phosphoglycolate in mammalian cells. Phosphoglycolate (A) and glycolate (B) levels were measured by GC/MS analysis in cell extracts 5 h after addition of 5 mM glycolate to parental HCT116 cells and a PGP knockout clone, as well as to cells that have been complemented by transduction with a retroviral construct driving expression of a mouse PGP cDNA or an empty control construct [18]. Values are relative to the wild type without glycolate addition and represent the mean ± s.e.m. of three independent experiments. Asterisks indicate $p < 0.05$ in post-hoc t-test analysis corrected for multiple testing.

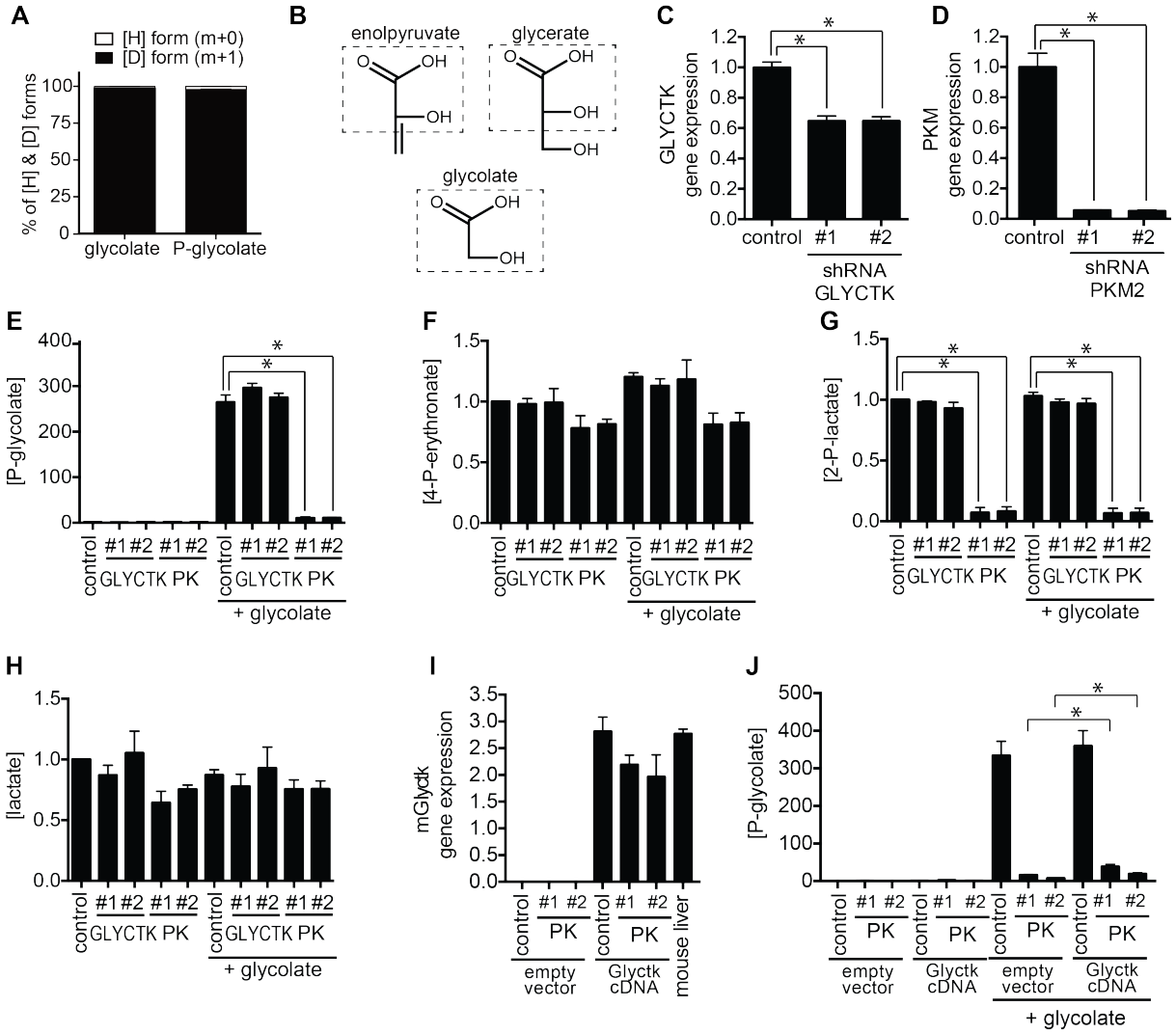

Figure 2. Phosphoglycolate is mainly formed by pyruvate kinase in the colorectal cancer cell line HCT116. A, Relative abundance of glycolate and phosphoglycolate isotopomers was assessed by GC/MS in PGP knockout HCT116 cells (and wild type cells, not shown) 6 h after treatment with 5 mM deuterated glycolate. Values shown represent the contribution of ^{1}H and ^{2}H after correction for the contribution of the trimethylsilyl part and the carbon backbone of glycolate. **B,** Similarity between glycerate, glycolate and enolpyruvate.

C - D, Relative gene expression of GLYCTK (**C**) and PKM2 (**D**) in cells treated with two different shRNAs.

E - H, Relative concentrations of phosphoglycolate (**E**), 4-P-erythronate (**F**), 2-P-lactate (**G**) and lactate (**H**) were measured by GC/MS in GLYCTK and PKM2 knockdown cell lines 6 h after addition of 5 mM glycolate. Values represent the mean ± s.e.m. of four independent experiments and were normalized within each experiment to untreated wild type cells.

I-J, We generated PGP knockout HCT116 cells where we knocked down PKM2 and overexpressed (or not) muring Glyctk mRNA. mRNA levels were assessed in these cell lines in comparison to mouse liver (**I**) and are represented normalized to the abundance of U6 mRNA (means +/- s.e.m., n=3).

Phosphoglycolate concentrations (**J**) were assessed in these cell lines and are presented normalized to untreated control cells within each experiment (means +/- s.e.m. of three independent experiments). Asterisks indicate $p < 0.05$ in post-hoc t-test analysis corrected for multiple testing.

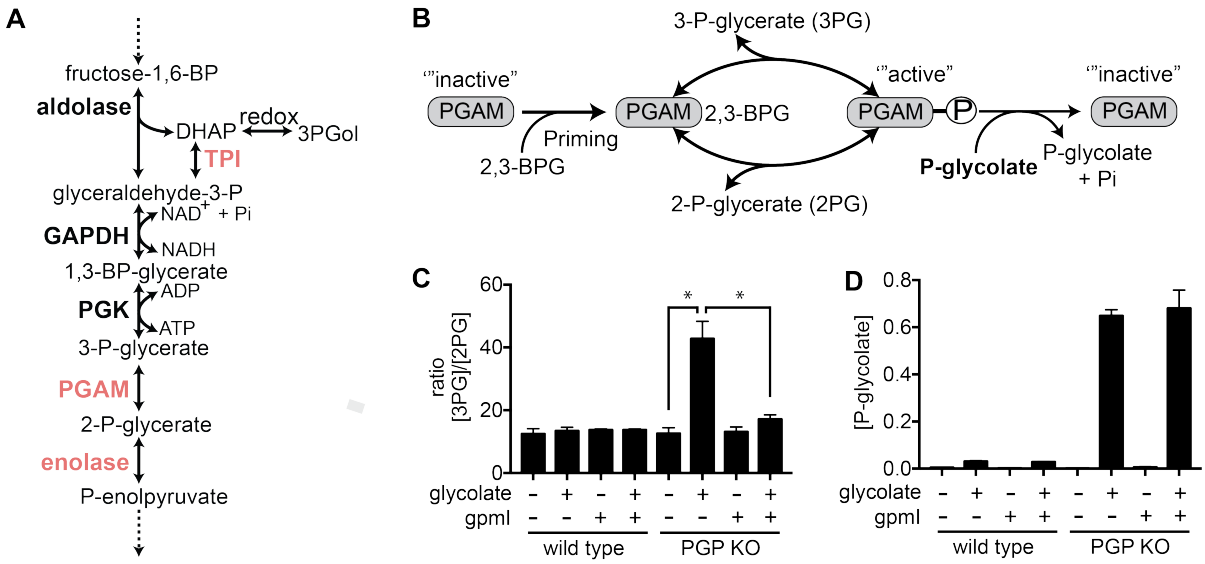

Figure 3. Phosphoglycolate accumulation blocks phosphoglycerate mutase – a process that can be prevented by expression of gpmI. A&B, Schematic representations of part of glycolysis (A) and the reaction catalysed by phosphoglycerate mutase in the absence or presence of phosphoglycolate (B). **C&D**, The ratios of 3-P-glycerate/2-P-glycerate concentrations (**C**) and phosphoglycolate concentrations (**D**) were assessed in parental HCT116 cells or in a PGP knockout clone expressing (or not) the 2,3-BPG-independent phosphoglycerate mutase, gpmI, from *Escherichia coli*. Values represent the mean ± s.e.m. of four independent experiments and are presented normalized to total ion current in arbitrary units. Asterisks indicate $p < 0.05$ in post-hoc t-test analysis corrected for multiple testing.

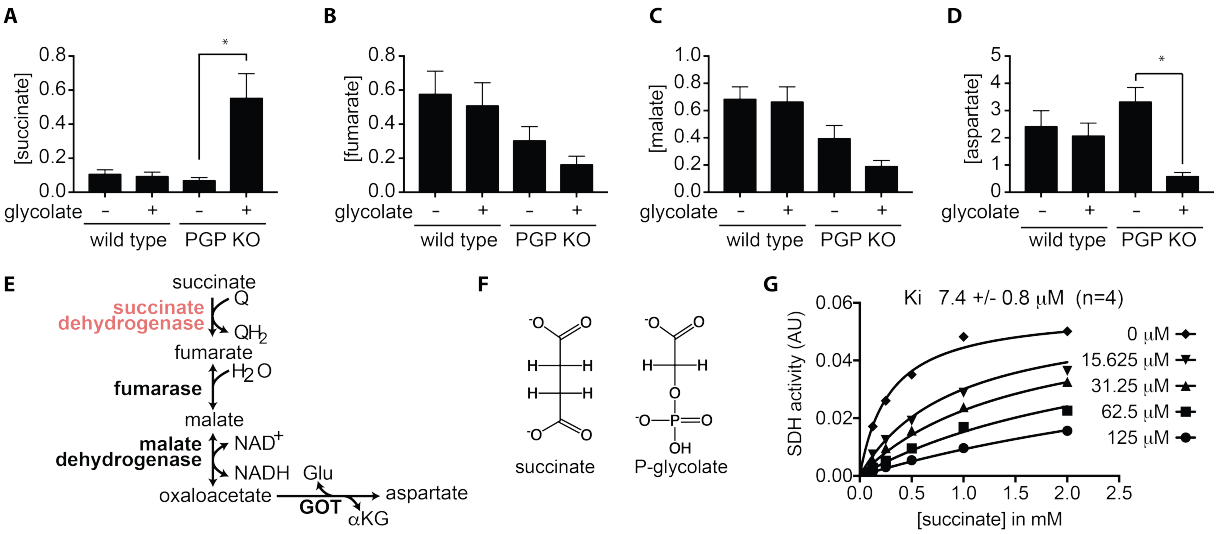

Figure 4. Phosphoglycolate blocks succinate dehydrogenase. A - D, Concentrations of succinate (**A**), fumarate (**B**), malate (**C**) and aspartate (**D**) were determined by GC/MS analysis of wild type or PGP knockout HCT116 cells in the presence or absence of 5 mM glycolate for 6h. Values represent the mean ± s.e.m. of four independent experiments and are presented normalized to total ion current in arbitrary units. Asterisks indicate $p < 0.05$ in post-hoc t-test analysis corrected for multiple testing. **E**, Schematic representation of the metabolites measured in panels A – D in the citric acid cycle. **F**, Structural similarity of phosphoglycolate and succinate. **G**, succinate dehydrogenase (SDH) activity of rat liver mitochondria was assessed in the presence of varying concentrations of phosphoglycolate and succinate. The Ki obtained from 4 independent experiments was 7.4 +/- 0.8 μM.

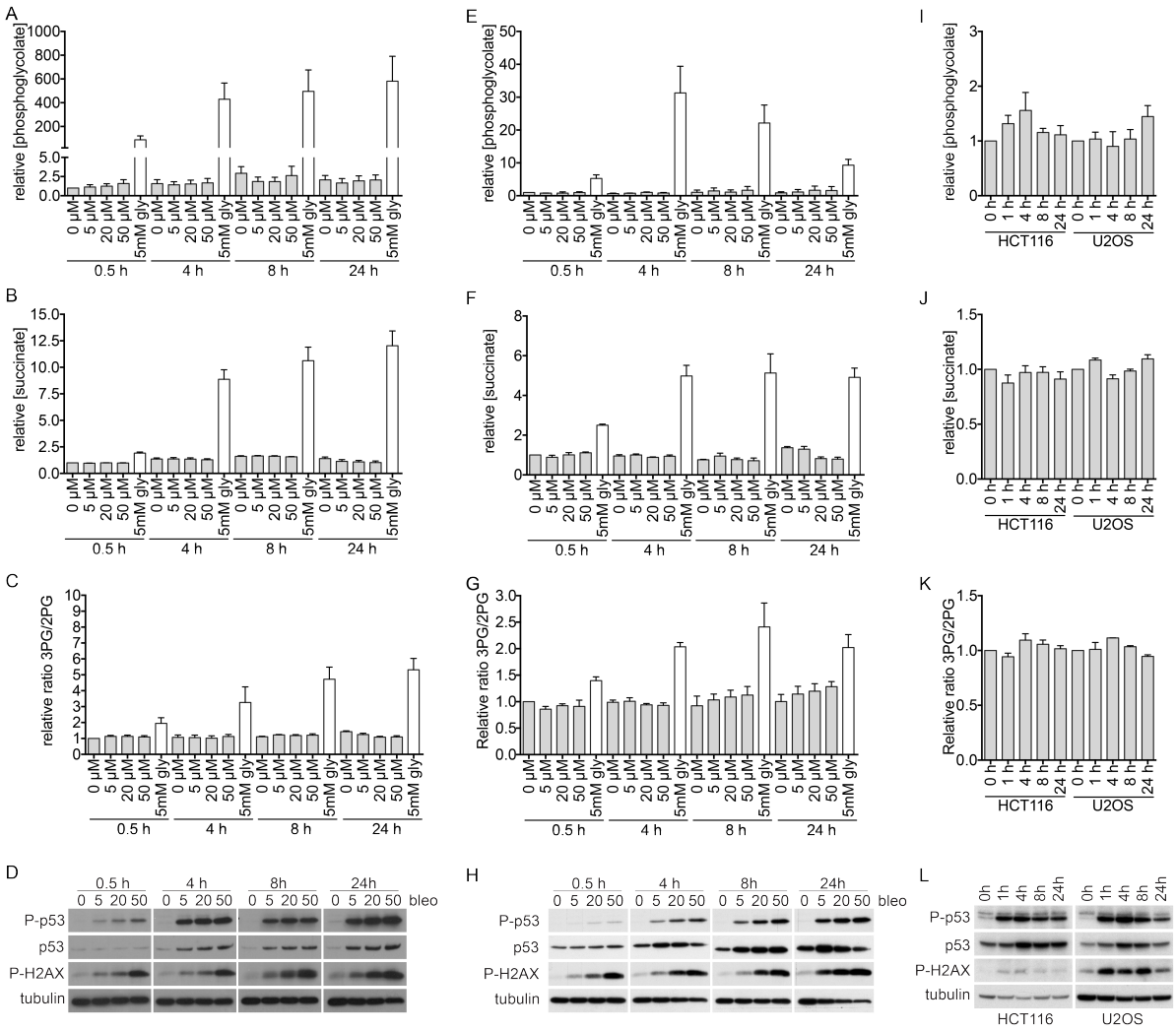

Figure 5. Phosphoglycolate concentrations observed upon DNA damage with Bleomycin are far from the concentrations that lead to metabolic effects. A - H, PGP knockout clones derived from the cell line HCT116 (A-D) and U2OS (E-H) were incubated for the indicated times with the indicated concentrations of Bleomycin, grey columns, or 5 mM glycolate, white columns. Using GC/MS, we analysed phosphoglycolate concentrations (**A&E**), succinate concentrations (as a measure of the inhibition of succinate dehydrogenase) (**B&F**), and the ratio of 3-P-glycerate/2-P-glycerate (as a measure of the inhibition of PGAM) (**C&G**). The cellular DNA damage response was assessed by western blot analysis using p53, phospho-p53 and phospho-H2AX antibodies. Equal loading was verified by hybridization with a β-tubulin antibody (**D&H**). Values represent the mean ± s.e.m. of three independent experiments and are normalized to the wild type untreated cells at 0.5h.

I-L, metabolite concentrations (**I-K**) and DNA damage markers (**L**) were assessed in PGP knockout clones obtained from the indicated cell lines at the indicated time points after 5 Gy irradiation. Data is presented as described in panels A-H.

SUPPLEMENTARY DATA

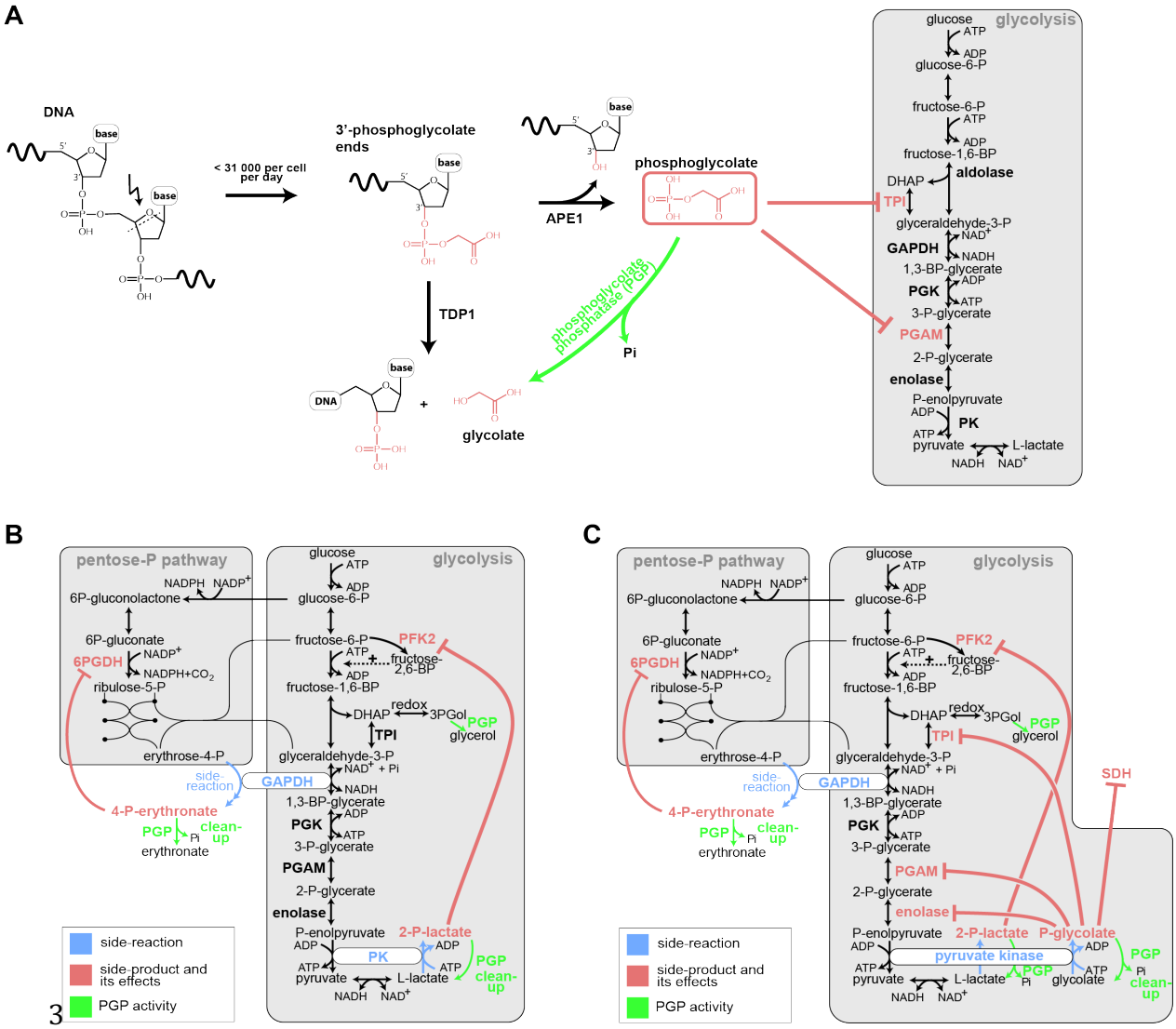

Supplementary Figure 1: Schematic representation of the pathways under investigation

A, Schematic representation of the link between DNA damage, phosphoglycolate and potential metabolic changes. Cleavage of the deoxyribose backbone can lead to the formation of 3' ends carrying phosphoglycolate groups. These 3'-phosphoglycolate ends are repaired either by removal of phosphoglycolate by the enzyme APE1 [3, 4] or by removal of glycolate by the enzyme TDP1 [5-7]. Phosphoglycolate is expected to be dephosphorylated by the enzyme phosphoglycolate phosphatase. Accumulation of phosphoglycolate could lead to an inhibition of triose phosphate isomerase (TPI) and, indirectly, of phosphoglycerate mutase (PGAM).

B, Schematic representation of a major metabolic clean-up function of the enzyme phosphoglycolate phosphatase revealed in previous work [18]. When the enzymes pyruvate kinase and glyceraldehyde 3-P dehydrogenase erroneously act on L-lactate and erythrose 4-P, they form 2-P-L-lactate and (indirectly) 4-P-erythronate, respectively. In normal cells, these side-products are rapidly dephosphorylated by the enzyme phosphoglycolate phosphatase. Yet, when this enzyme is absent, we observed a strong increase in these metabolic side products. We also observed more than 50-fold increases in 6P-gluconate concentrations, most likely due a very efficient inhibition of the enzyme 6P-gluconate dehydrogenase (6PGDH) by 4P-erythronate. Furthermore, we observed a reduction of glycolytic flux, which is most likely at least in part caused by the inhibition of phosphofructokinase-2 by L-2-P-lactate [18].

In addition, several papers described increases of 3P-glycerol (3PGol) when PGP is knocked down or knocked out [15, 19, 20]. Yet, it should be noted that the catalytic efficiency for this metabolite is ≈ 100x lower than the one for phosphoglycolate, 2-P-L-lactate and 4-P-erythronate[18].

C, Schematic representation of biogenesis and metabolic effects of phosphoglycolate observed in the present work.

Phosphoglycolate in our experimental system is largely synthesized by phosphorylation of glycolate. High concentrations of phosphoglycolate can lead to an inhibition of triose phosphate isomerase, phosphoglycerate mutase, enolase and succinate dehydrogenase (SDH).

BP, bisphosphate; P, phosphate; 6PGDH, 6P-gluconate dehydrogenase; PFK2, phosphofructokinase 2; 3PGol, 3P-glycerol; P-glycolate, phosphoglycolate; DHAP, dihydroxyacetone phosphate; PGK, phosphoglycerate kinase; PGP, phosphoglycolate phosphatase; TPI, triose phosphate isomerase; PGAM, phosphoglycerate mutase; PK, pyruvate kinase; SDH, succinate dehydrogenase. Not all cofactors are listed.

The word “redox” in the reaction between dihydroxyacetone phosphate (DHAP) and 3P-glycerol (3PGol) indicates that this reaction is determined both by the cytoplasmic NADH/NAD^+ ratio and the ratio of reduced to oxidized coenzyme Q.

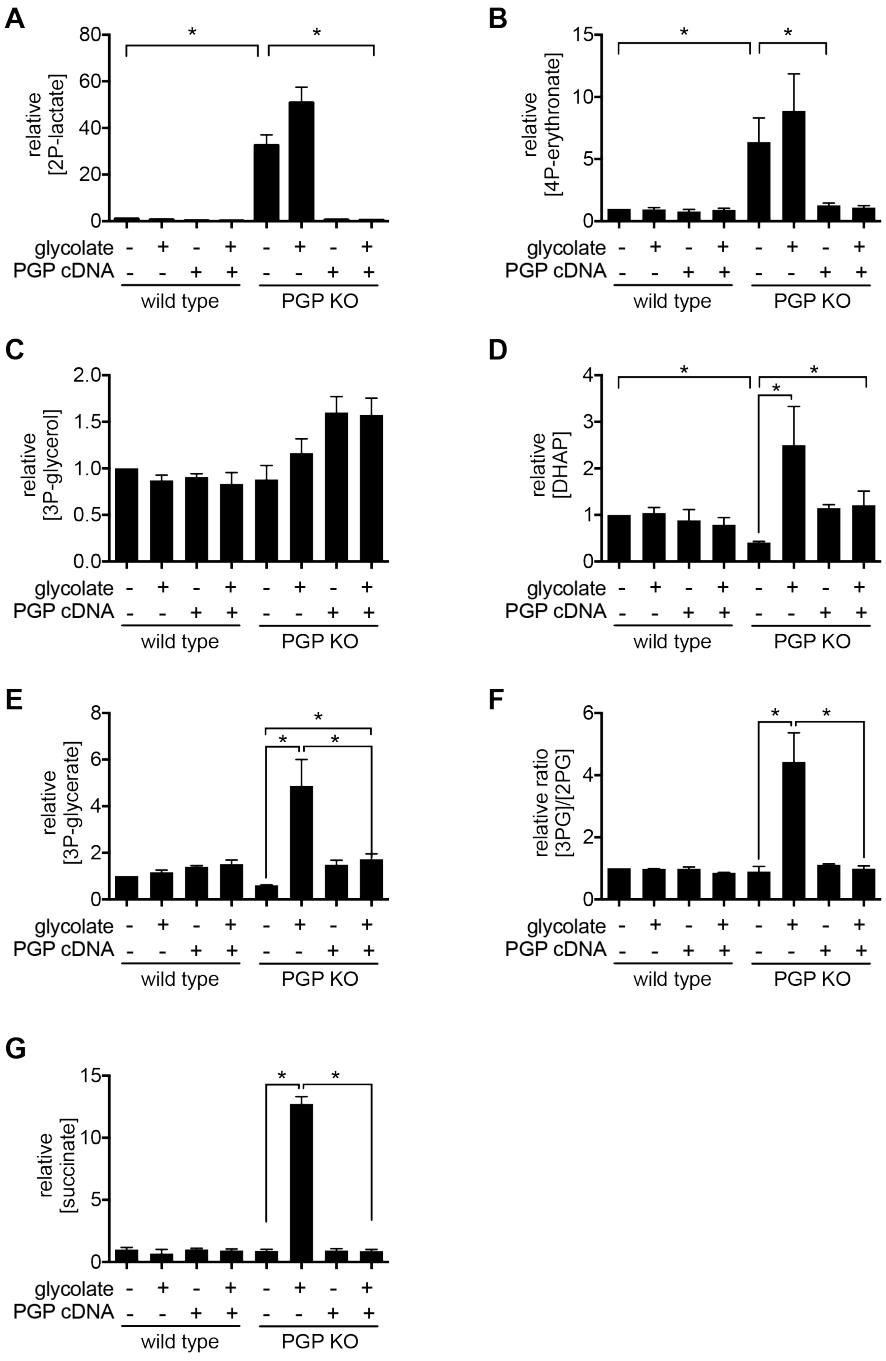

Supplementary Figure 2. Relative metabolite content of cells described in Figure 1. Concentrations have been assessed by GC/MS in parental HCT116 cells or in a PGP knockout clone after treatment or not with glycolate. Cell lines were either transduced with a retroviral construct driving expression of mouse PGP cDNA ("+") or an empty control construct ("-"). Values represent the mean ± s.e.m. of three independent experiments and are presented relative to the untreated wild type cells.

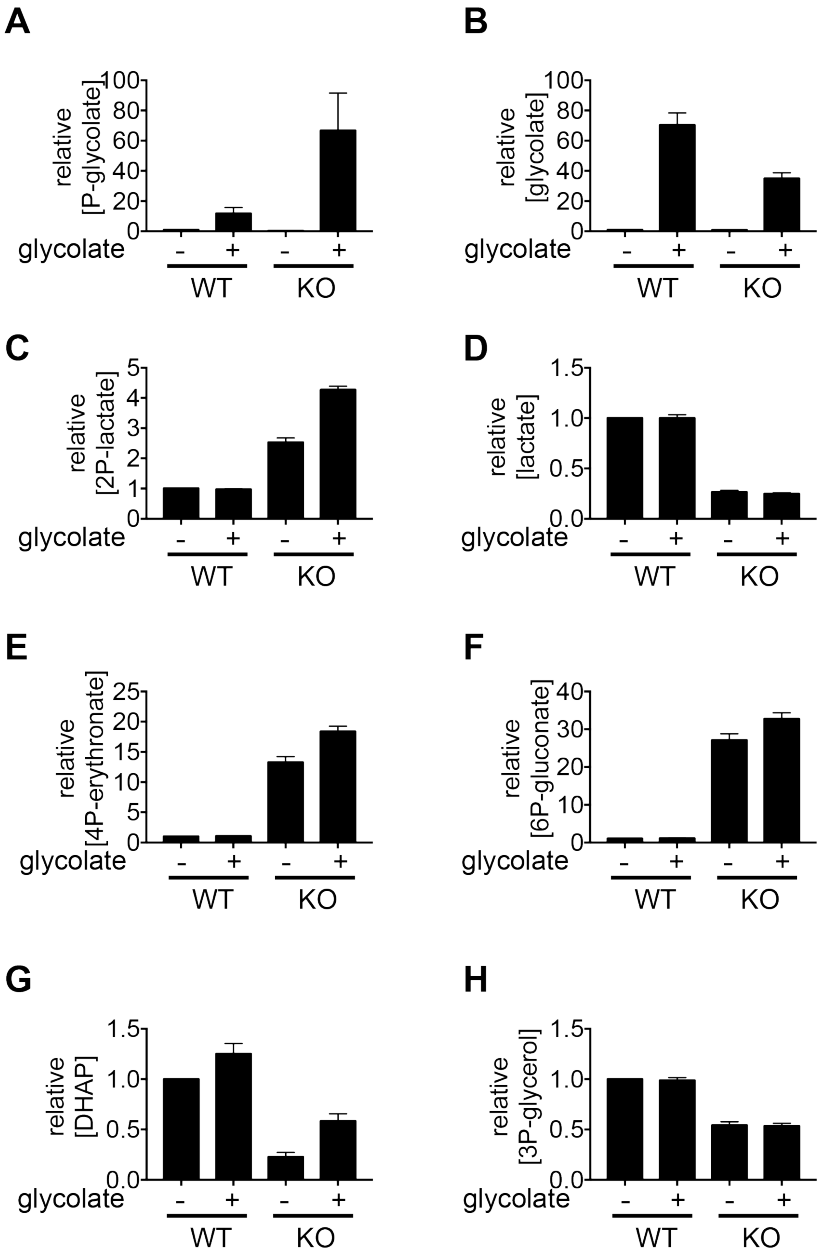

Supplementary Figure 3. Relative metabolite content of wild type and PGP knockout U2OS cells in the presence and absence of glycolate treatment. Concentrations of phosphoglycolate (A), glycolate (B), 2P-lactate (C), lactate (D), 4P-erythronate (E), 6P-gluconate (F), dihydroxyacetone phosphate (DHAP) (G) and 3P-glycerol (H) were measured by GC-MS and were normalized to the untreated wild type cells within each experiment. Values represent means ± s.e.m. of four independent experiments and are presented relative to the untreated wild-type cells..

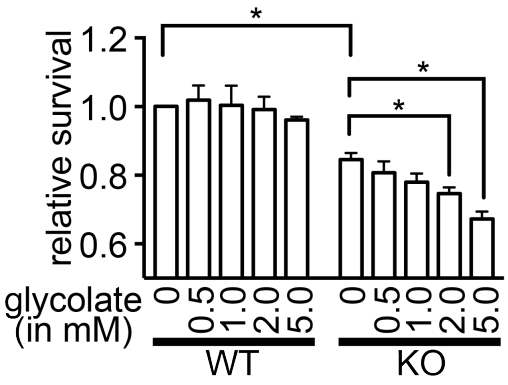

Supplementary Figure 4: Survival of wild type and PGP knockout cells in the presence of glycolate.

HCT116 wild type and PGP knockout cells were plated in the presence of the indicated concentrations of glycolate. Viability was assessed with the Alamar blue assay 1 and 4 days after plating. The signal obtained at day 4 was normalized to the one obtained at day 1 to correct for differences in plating. Values are means +/- s.e.m. of four independent experiments performed in 6 replicates, and are presented relative to the untreated wild type cells.

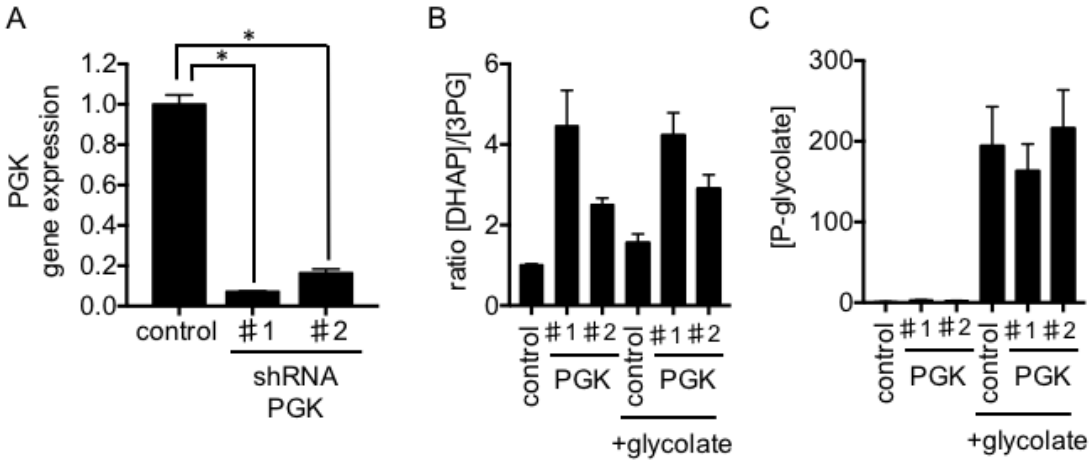

Supplementary Figure 5. Phosphoglycerate kinase does not contribute to the formation of phosphoglycolate.

A, Phosphoglycerate kinase 1 mRNA levels (relative to U6) were assessed by qPCR in HCT116 PGP knockout clone C4 expressing a non-silencing control shRNA or two independent shRNAs targeting human PGK1. Values represent means and s.e.m. from three independent experiments. **B&C,** Dihydroxyacetone phosphate (DHAP), 3-phosphoglycerate (3PG) (expressed as concentration ratios in **B**) and phosphoglycolate concentrations (**C**) were determined by GC-MS in the cell lines described in A after incubation or not with glycolate. Values were normalized to those obtained in untreated control shRNA expressing cells in each experiments and represent the means +/- s.e.m. of three independent experiments.

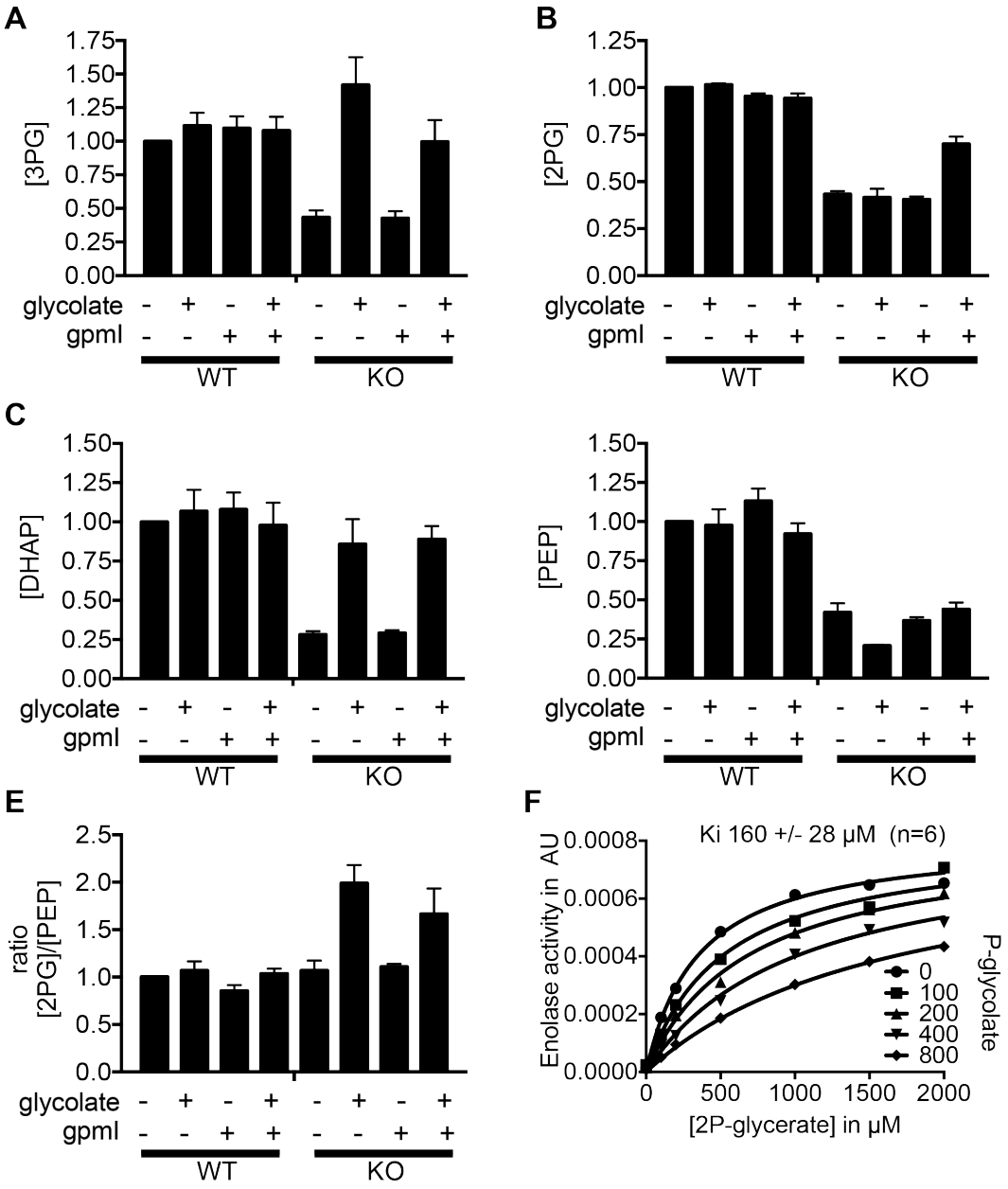

Supplementary Figure 6. Relative metabolite content of cells described in Figure 3.

A-E Concentrations are relative to the untreated wild type cells and have been assessed in parental HCT116 cells or in a PGP knockout clone expressing (or not) the 2,3-BPG-independent phosphoglycerate mutase gpmI from *Escherichia coli*. Values represent the means ± s.e.m. of four independent experiments and are presented relative to the untreated wild-type cells. **F,** Enolase activity was assessed in the presence of the indicated concentrations of phosphoglycolate (in μM). Curves were fit using Prism 7. The presented Ki is the mean +/- s.e.m. of six independent experiments.

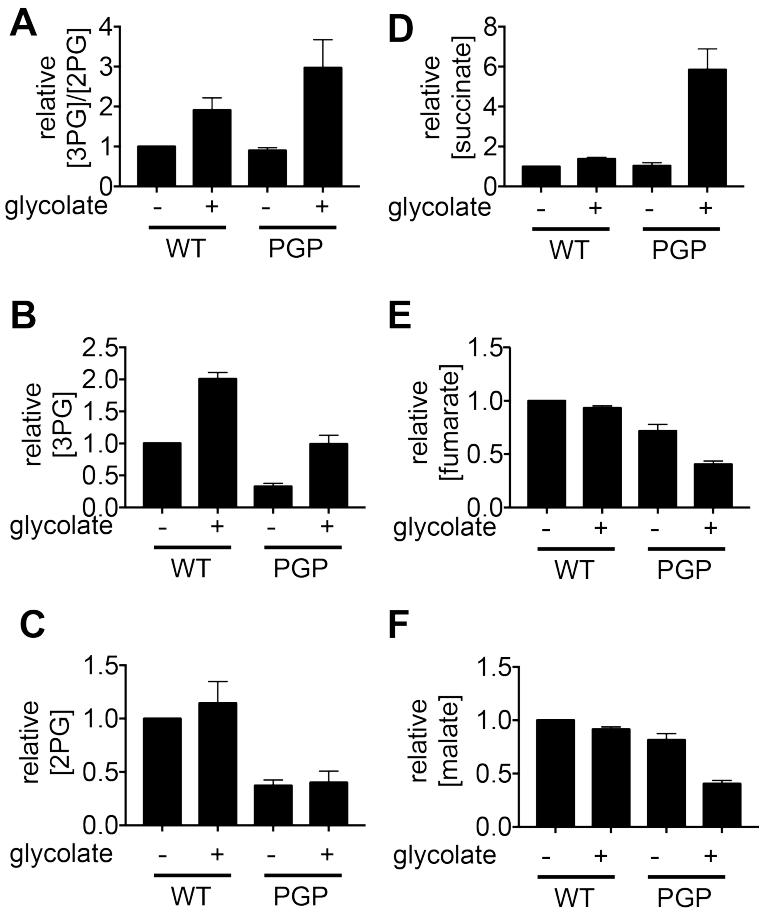

Supplementary Figure 7. Relative metabolite content in wild type and PGP knockout U2OS cells in the presence and absence of glycolate treatment.

The ratio of 3PG to 2PG (A), as well as 3-P-glycerate (3PG) (B), 2P-glycerate (2PG) (C), succinate (D), fumarate (E) and malate (F) were measured by GC-MS and were normalized to the untreated wild type cells within each experiment. Values represent means ± s.e.m. of four independent experiments.

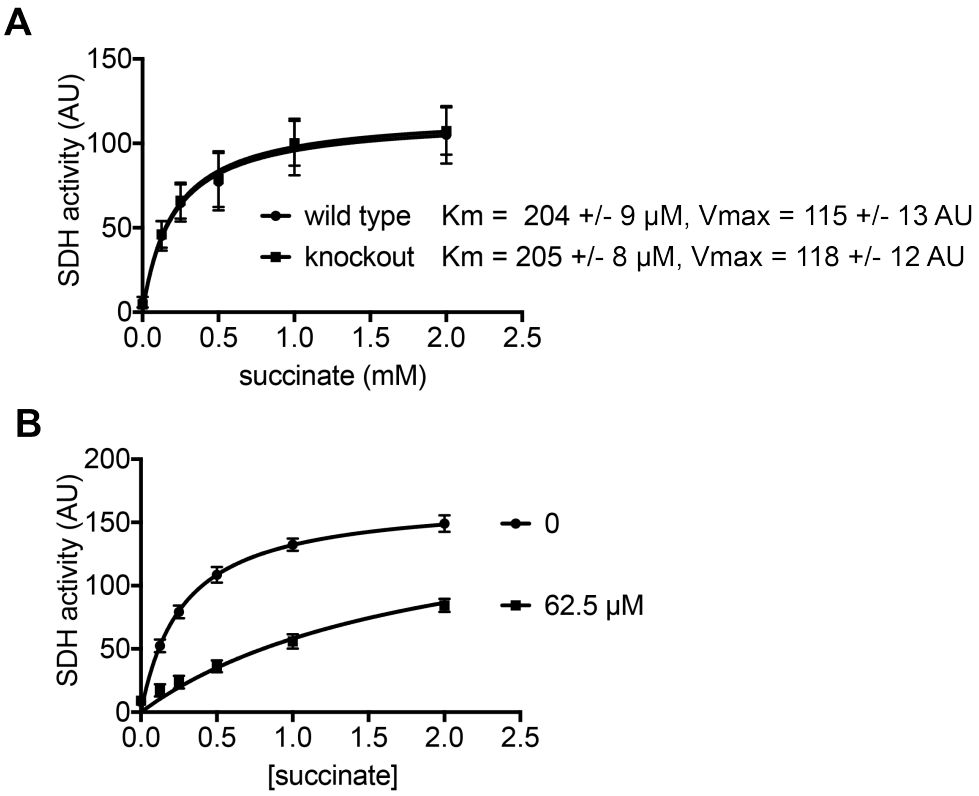

Supplementary Figure 8. Succinate dehydrogenase activity in extracts from HCT116 cells and its inhibtion by phosphoglycolate.

A, Succinate dehydrogenase (SDH) activity was determined in cellular extracts obtained from PGP wild type or knockout HCT116 cells. Estimates of Km and Vmax are means +/- s.e.m. (n=3).

B, Succinate dehydrogenase activity in PGP knockout HCT116 cells was determined in the presence or absence of 62.5 μM phosphoglycolate.

Presented values were normalized to protein concentrations and means +/- s.e.m. (n=3).

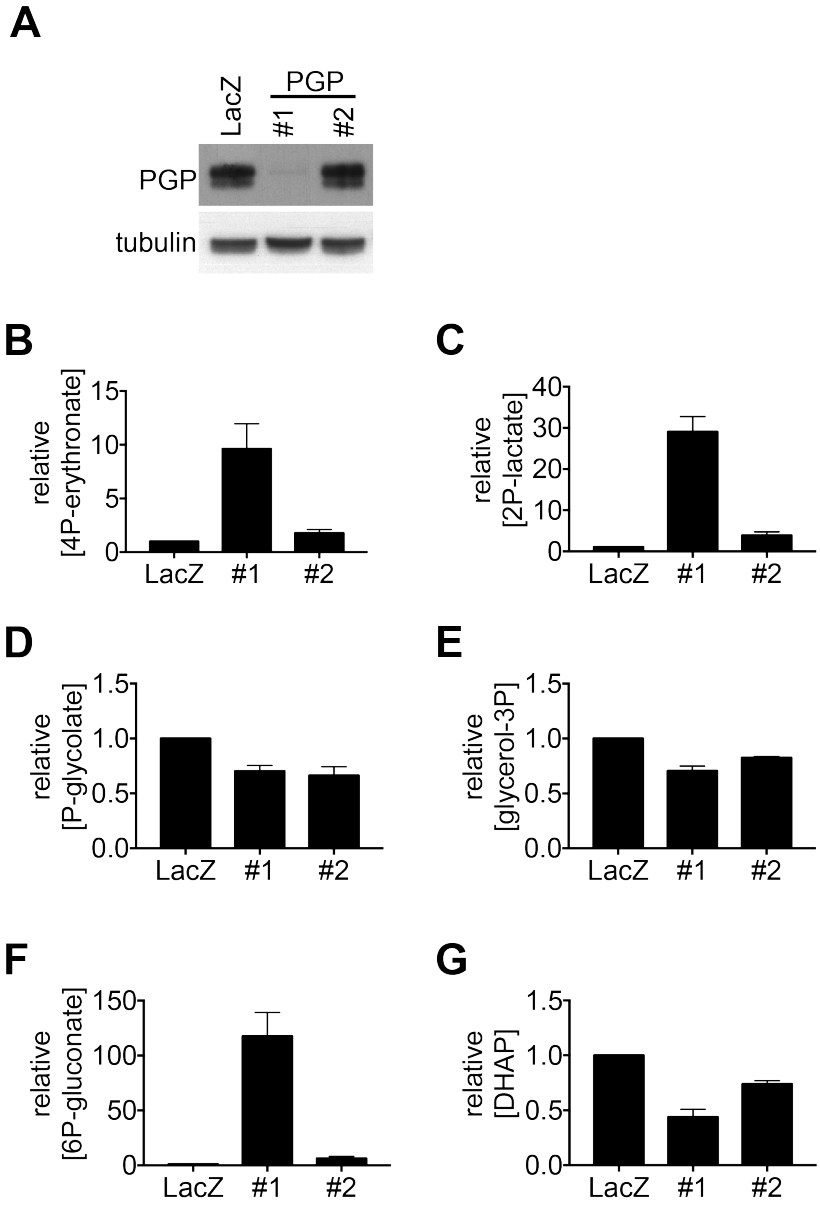

Supplementary figure 9: Metabolite changes in PGP-mutant human fibroblasts

A, Western blot analysis of immortalized human HFF2 fibroblasts upon lentiviral transduction with CRISPR/Cas9 constructs driving expression of a guide RNA targeting LacZ ("WT") or two guide RNAs targeting human PGP ("#1" and "#2"). As can be seen in this panel, polyclonal expression of guide-RNA #2 only leads to a minimal reduction of PGP levels, whereas guide RNA #1 leads to a knockout in almost all cells.

B-G, Metabolite concentrations were assessed by GC-MS in the indicated polyclonal cell lines and were normalized to the untreated wild type cells within each experiment. Values represent mean ± s.e.m. of four independent experiments.

1

Supplementary Table 1: Primers used in the current study

hGLYCTK_1	TGC TGT TGA CAG TGA GCG CCA CCC TGT TTC TTT CTG TGA ATA GTG AAG CCA CAG ATG TAT TCA CAG AAA GAA ACA GGG TGA TGC CTA CTG CCT CGG A
hGLYCTK_2	TGC TGT TGA CAG TGA GCG CGC CAT GCA AGG TGA TGT AAA ATA GTG AAG CCA CAG ATG TAT TTT ACA TCA CCT TGC ATG GCT TGC CTA CTG CCT CGG A
hPKM_1	TGC TGT TGA CAG TGA GCG CGC CTA CCT GTA TGT CAA TAA ATA GTG AAG CCA CAG ATG TAT TTA TTG ACA TAC AGG TAG GCT TGC CTA CTG CCT CGG A
hPKM_2	TGC TGT TGA CAG TGA GCG CCT GTC CAG TTC CTT TAG AAA ATA GTG AAG CCA CAG ATG TAT TTT CTA AAG GAA CTG GAC AGA TGC CTA CTG CCT CGG A
hPGK1_1	TGC TGT TGA CAG TGA GCG ATG CTG ACA AGT TTG ATG AGA ATA GTG AAG CCA CAG ATG TAT TCT CAT CAA ACT TGT CAG CAG TGC CTA CTG CCT CGG A
hPGK1_2	TGC TGT TGA CAG TGA GCG CTG GCA CTT CTC TGT TTG ATG ATA GTG AAG CCA CAG ATG TAT CAT CAA ACA GAG AAG TGC CAA TGC CTA CTG CCT CGG A
Q_mGLYCTK_s	CTG CGG GAA AAC CTC TAC CTA
Q_mGLYCTK_as	CGA TCC GGT AAG TTG TCC TCG
Q_U6_s	CGC TTC CGC AGC ACA TAT AC
Q_U6_as	TTC ACG AAT TTG CGT GTC AT
Q_PGK1_s	TGGACGTTAAAGGGAAGCGG
Q_PGK1_as	GCTCATAAGGACTACCGACTTGG
PGP_guide1_s	CAC CGG CAG CGG GCG TCG TCG CCA C
PGP_guide1_as	AAA CGT GGC GAC GAC GCC CGC TGC C
PGP_guide2_s	CAC CGG CGG CGC TCA GCC GCA CGC AG
PGP_guide2_as	AAA CCT GCG TGC GGC TGA GCG CCG CC

Supplementary Table 2. GC/MS analysis of metabolites

	Quantifyer m/z	**Qualifyer m/z**
glycolate	205 (206 for D)	
phosphoglycolate	357 (358 for D)	328
2-P-lactate	371	299
4-P-erythronate	357	561
3-P-glycerate	315	299, 387

2-P-glycerate	315	299, 387
succinate	247	129
fumarate	245	83
malate	233	335
aspartate	232	218
PEP	369	384
DHAP	315	299, 387
glucose-6-P	357	299, 315, 459
6-P-gluconate	387	315, 357
fructose-6-P	357	299, 315, 459
glycerol-3-P	357	387

1

2